

# SOVIET PHYSICS USPEKHI

*A Translation of Uspekhi Fizicheskikh Nauk*

SOVIET PHYSICS USPEKHI

Russian Vol. 75, Nos. 1-2

MARCH-APRIL 1962

## POSSIBLE INVESTIGATION OF RELATIVISTIC EFFECTS WITH THE AID OF MOLECULAR AND ATOMIC FREQUENCY STANDARDS

N. G. BASOV, O. N. KROKHIN, A. N. ORAEVSKII, G. M. STRAKHOVSKII, B. M. CHIKHACHEV  
Usp. Fiz. Nauk **75**, 3-59 (September, 1961)

Introduction . . . . .	641
I. Atomic and Molecular Frequency and Time Standards . . . . .	642
1. Molecular and Atomic Generators . . . . .	642
2. Cesium Frequency Standards . . . . .	647
3. Other Frequency Standards . . . . .	649
4. Frequency Stabilization . . . . .	651
II. Use of Highly Stable Frequency and Time Standards to Check General and Special Relativity . . . . .	653
1. Possible Experiments to Check General Relativity . . . . .	653
2. First-Order Experiments to Check Special Relativity . . . . .	666
III. Use of Atomic and Molecular Frequency Standards for the Investigation of Cosmological Effects . . . . .	669
Conclusion . . . . .	670
Appendix. Derivation of Formula for Relativistic Red Shift of the Frequency of a Spectral Line . . . . .	670
References Cited . . . . .	671

### INTRODUCTION

DURING the last decade much progress was made in the development of highly stable molecular and atomic frequency (time) standards. The frequency reference in such standards is the natural frequency of a spectral line, and consequently such standards, unlike quartz standards, are absolute and need no constant monitoring against astronomic observations.

At present two types of frequency standards are in principal use, the maser and the cesium frequency standard. Frequency (time) standards based on masers are called molecular standards, while those using the spectral lines of cesium atoms are called atomic. The two differ essentially in their operating principle, construction, etc., but compete successfully with each other, giving a comparable measurement accuracy, at present on the order of about  $10^{-10}$ . The accuracy of such standards can be increased by various methods to  $10^{-11} - 10^{-12}$  (see references 29 and 110).

Most recently a group of physicists headed by N. Ramsay succeeded in constructing a highly stable atomic generator using a beam of hydrogen atoms<sup>101</sup> (radiated wavelength  $\sim 21$  cm).

Masers are self-oscillating systems, emitting highly monochromatic oscillations, whereas cesium standards are only high-Q discriminators and require

the use of a separate and independent, usually crystal-controlled, oscillator. Masers can therefore generate very stable frequencies. The mentioned  $10^{-10}$  accuracy refers to the possibility of tuning the generator to the frequency of a spectral line, that is, to absolute stability. There are masers in existence in which the relative change in frequency is less than  $10^{-11}$  in six hours, and amounts to  $10^{-13} - 10^{-14}$  during a time on the order of a second.<sup>28,111</sup>

The high accuracy of molecular and atomic standards has made it possible to solve many important physical and technical problems. The use of atomic and molecular instruments increases greatly the accuracy and sensitivity of radar devices.<sup>112</sup> Great possibilities are afforded to the frequency and time services. Astronomers can study anew the motion of celestial bodies with clocks that operate independently of this motion. Irregularities in the earth's rotation have already been observed and steps made toward their systematic study. Work began on comparison of "astronomic" clocks with "atomic" or "molecular" ones.

The high accuracy with which the frequencies of spectral lines can be measured with atomic and molecular instruments permits the use of these instruments as radiospectroscopes of very high resolution. This permits a precision measurement of molecular and nuclear constants, which are very valuable for the

theory of the chemical bond and for nuclear physics.

Masers were used to check experimentally on the theory of relativity; in particular, measurements of first-order relativistic effects with apparatus of the type used by Michelson have been made with a thousand-fold accuracy compared with optical measurements. Many different methods have been proposed to measure the gravitational frequency shift in the general theory of relativity. Although much progress has recently been made in this field through the use of very narrow lines in nuclear decays,\* so that it is possible<sup>1</sup> to measure the gravitational frequency shift predicted by the general theory of relativity with accuracy up to 4 percent, such measurements have not lost their urgency. Molecular instruments can be carried by satellites and space rockets to great distances away from the earth, thereby yielding considerable gravitation frequency shifts and permitting measurements with a greater degree of accuracy.

Various effects connected with the structure of the universe, now under discussion, can be measured with molecular and atomic instruments. It has been pointed out, for example, that the reading of an atomic clock should differ measurably from that of a molecular clock because the "expansion" of the universe will influence differently the physical constants on which the operation of atomic and molecular standards are based.

The possibility of investigating effects of screening of the gravitational field<sup>3,10</sup> is being studied with the aid of atomic and molecular instruments.

The greatest difficulties in setting up measurements of gravitational effects with the aid of atomic and molecular frequency standards carried by satellites or space rockets are due to the first-order Doppler effect caused by the motion of the satellite or the rocket, since the first-order Doppler frequency shift exceeds by  $10^4 - 10^5$  the gravitational frequency shift. Many methods for compensating for the first-order Doppler effect were proposed.

This method makes feasible experiments with satellite-borne masers to check the effect of general relativity with a high degree of accuracy. In reference 4 it was proposed to carry out not frequency measurements but comparisons of sufficiently long time intervals, measured with satellite-borne and earth-based clocks. Such experiments do not completely eliminate the first-order Doppler effect, however, since they necessitate a very precise knowledge of the coordinates at the instant when the satellite radiates the time signal.

It was proposed<sup>5</sup> to compensate for the first-order Doppler effect by transmitting a frequency from the

earth to a satellite and from the satellite to the earth, with suitable frequency conversion on the satellite. Such an experimental setup would simultaneously get rid of the first-order Doppler frequency shift and double the gravitational frequency shift. The difficulty in the practical realization of such schemes is that the transmission and reception are at close frequencies, making pulsed operation necessary. Operation at different frequencies is feasible, but the influence of the ionosphere is then intensified.

The foregoing scheme for doubling the gravitational phase shift, through transmission of a signal from the earth to the satellite and back, admits of the following generalization: in multiple signal propagation it is possible to increase the gravitational shift by a factor  $n$ , equal to the number of paths covered by the signal from the earth to the satellite and from the satellite to the earth. Multiple passage of the signal can be used for experiments under terrestrial conditions, with one generator mounted on the earth's surface and the other at some height. It is necessary here that the change in the generator frequency during the time of measurement be smaller than the gravitational shift, this being ensured by the high relative stability of the maser frequency.

In the present article we review papers devoted to possible experiments, using highly stabilized molecular and atomic frequency standards, aimed at verifying the general theory of relativity, certain questions in the special theory of relativity, and some cosmological hypotheses. We begin with a brief review of work on molecular and atomic frequency standards and on methods of stabilization of radio-frequency oscillators with the aid of such standards. This brief review, which discusses general problems connected with the principal methods used to produce frequency standards, as well as many specific circuits, problems treated in a large number of foreign and domestic papers, will be particularly useful to a reader who has not specialized in quantum radiophysics.

Many papers have been devoted to the various theoretical aspects of the general theory of relativity. A detailed analysis of many effects of general relativity, the possible experimental verification of which is discussed in the present review, and many new interesting consequences which can be subjected to experimental analysis, are found in an article by V. L. Ginzburg.<sup>6</sup> We therefore pay principal attention in the present article not to a theoretical analysis of relativistic and gravitational effects, but to the possibilities of setting up various experiments to study these effects, and also to a verification of certain cosmological hypotheses with the aid of new high-stability molecular and atomic frequency standards.

## I. ATOMIC AND MOLECULAR FREQUENCY AND TIME STANDARDS

### 1. Molecular and Atomic Generators

The first molecular generator (maser) developed<sup>7,8</sup> used the inversion spectrum of the ammonia molecule  $N^{14}H_3$ .

\*Mössbauer<sup>2</sup> was able to demonstrate theoretically and experimentally that under certain conditions the spectral lines of nuclei situated in a crystal lattice are not broadened by recoil upon emission of a photon, since the recoil momentum is taken up not by the nucleus but by the crystal as a whole, and consequently the width of the spectral line is determined essentially by the lifetime of the radioactive nucleus. Spectral lines with relative width  $\sim 10^{-12} - 10^{-15}$  were obtained experimentally.<sup>1,2</sup>

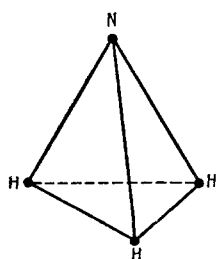


FIG. 1. Geometric structure of ammonia molecule.

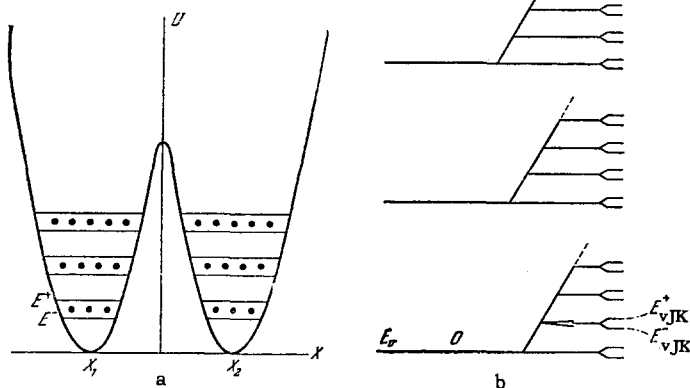


FIG. 2. a) Dependence of the potential energy  $E$  of the ammonia molecule  $\text{NH}_3$  on the distance ( $X$ ) between the atom of the nitrogen and the plane passing through the hydrogen atoms, and inversion-level scheme of the non-rotating molecule:  $E^+$  – upper inversion level,  $E^-$  – lower inversion level,  $X_1$  and  $X_2$  – coordinates of two equilibrium configurations of the molecule. The inversion levels of the ammonia are added to the rotational levels and depend on the rotational quantum numbers  $J$  and  $K$ . b) Energy level scheme of  $\text{NH}_3$  molecule. To each vibrational energy level  $E_v$  there is added an infinite number of levels  $E_{vJK}$ , due to the rotation. The latter are in turn split into two inversion levels,  $E_{vJK}^+$  being the upper and  $E_{vJK}^-$  the lower.

Ammonia is a symmetrical-top molecule similar in form to a regular pyramid, with the hydrogen nuclei at the vertices of the base and the nitrogen nucleus at the vertex of the pyramid (Fig. 1). The pure rotational spectrum of ammonia lies in the 7 mm band ( $\lambda < 0.1$  mm). A feature of the spectrum of  $\text{NH}_3$  is the splitting of each rotational level\*  $JK$  into two inversion sublevels (Fig. 2), with transition frequencies that lie in the well studied microwave band, and with inversion lines of sufficiently high intensity. It is these two factors that have contributed to the extensive use of ammonia for radiospectroscopic investigation in general and for the development of the maser in particular.†

The operation of the maser is based on the principle of induced emission from excited molecules.<sup>9</sup>

Usually the maser employs molecular beams,<sup>9</sup> although beamless systems are also possible.<sup>10</sup> The use

\*The quantum number  $J$  represents the rotational momentum of the molecule;  $K$  is the projection of this momentum on the symmetry axis of the molecule.

†More detailed information on the structure of the  $\text{NH}_3$  molecule and its spectrum can be found in books on radiospectroscopy.<sup>104, 105</sup>

of molecular beams makes it possible to solve two problems: it is possible to obtain with the aid of a molecular beam a sufficiently narrow spectral emission line; this, as will be shown later, is very important for high-frequency stability both in the maser and in the cesium standard; the molecular beam makes it possible to sort molecules by energy states and to obtain excited molecules with the aid of an inhomogeneous static electric or magnetic field.

The construction of an ammonia-beam maser is shown in Fig. 3a. The source of the molecular beam is a small cavity, in one of the walls of which is mounted a "sieve" with small openings, made of foil. In the maser developed in the Physics Institute of the Academy of Sciences a sieve was used in which the ratio of the total area of the holes to the total foil area was one-quarter, and in which the hole diameter was 0.05 cm. Other molecular-beam sources are also possible.<sup>11, 12</sup> In particular, narrow beams are obtained with channels having a length to diameter ratio ( $L/D$ ) greater than unity.

To obtain a beam of excited molecules, the ammonia molecules are sorted in an inhomogeneous electric field. This sorting is based on the fact that the energy of an ammonia molecule in the upper inversion level increases in an electric field, while the energy of the molecule in the lower inversion level decreases in an electric field. Consequently, when the molecules in the upper inversion level pass through a capacitor they are acted upon by a force directed toward the minimum of the electric field, while the force acting on the molecules in the lower inversion level is directed toward the maximum of the electric field. Thus, an inhomogeneous electric field can sort out the molecules in the upper and lower inversion levels. Usually a quadrupole capacitor is used for this purpose,<sup>7, 18, 13</sup> in which the electric field is zero on the axis and increases with increasing distance from the axis, thus causing focusing of the ammonia molecules that are at the upper inversion energy levels.

Along with a quadrupole capacitor, other systems with inhomogeneous electric fields<sup>14, 15</sup> can be used to sort the molecules by states. The system of coaxial rings (ring capacitor) described in reference 15 competes successfully with the quadrupole capacitor.

The emission from the molecules in the maser occurs in a metallic cavity, in which the passing molecules give up their energy as they go from the excited to the lower level. The molecular transitions occur under the influence of the field stored in the cavity as a result of the energy radiated by the preceding molecules. Thus, the feedback, which is necessary for any self-oscillating system, is produced in the maser by the field energy stored in the cavity. The nonlinearity that limits the growth of the oscillations in the cavity is due to saturation, the theory of which is given in references 16 and 17.

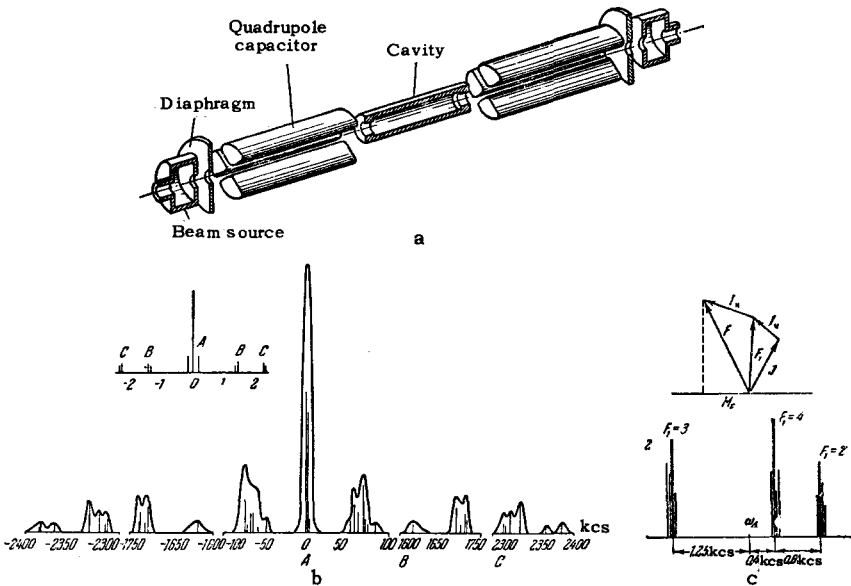


FIG. 3. a) Arrangement of two-beam maser. b) Structure of  $J=3, K=3$  ammonia line. c) Structure of central line  $J=3, K=3, \Delta F_1 = \Delta F = 0$ .<sup>26</sup>

The natural frequency of the resonator should be equal to the emission frequency of the molecules, so as to improve the self-excitation conditions and to obtain maximum absolute stability. The cavity frequency is determined by its geometric dimensions and by the mode excited in it.<sup>18</sup> The most useful is the  $E_{010}$  mode.<sup>8-19</sup> The choice of this mode is dictated by the fact that the electric field corresponding to the  $E_{010}$  mode is homogeneous along the cavity, and consequently there will be no Doppler broadening of the spectral line in the field of such a mode if the beam of incoming molecules is parallel to the cavity axis.<sup>9</sup> The presence of a slight angular spread in the real molecular beam does bring about a Doppler broadening of the spectral line, but if the  $E_{010}$  mode is excited in the cavity, this broadening is small. For example, if the beam angle is  $10^\circ$ , the relative Doppler broadening  $\Delta\nu_{\text{Dop}}/\nu$  is on the order of  $10^{-7}$ .

It is possible to excite the maser in a different mode,<sup>7</sup>  $H_{011}$ , in which the field is inhomogeneous along the cavity. In this case the diameter of the resonator should be close to critical, so that the inhomogeneity of the field along the resonator be insignificant and the Doppler broadening it produces does not exceed the width due to the finite transit time of the molecules through the cavity.

Production of a molecular beam calls for a high vacuum, about  $10^{-6}$  mm Hg.

The main feature of the maser as a time (frequency) standard is its stability. An investigation of the stability of the maser frequency as a function of the apparatus parameter is therefore an important step in the design of apparatus of high stability.

Even in the early work on maser theory it became clear that the maser frequency depends on the natural frequency of the cavity, on its  $Q$ , and on the  $Q$  of the spectral line. Calculations under the assumption that

1) the resonator can be replaced by a lumped-parameter circuit and 2) the emission line has a Lorentz shape (corresponding to a distribution  $\frac{1}{\tau} e^{-\tau/\bar{\tau}}$  for the molecule transit times) yield the following formula for the maser frequency<sup>20,21,22</sup>

$$\nu = \nu_{\Lambda} \left[ 1 - \frac{\nu_{\Lambda} - \nu_0}{\nu_{\Lambda}} \frac{Q}{Q_{\Lambda}} \right], \quad (1.1)$$

where  $\nu_{\Lambda}$  is the frequency of the spectral line,  $\nu_0$  the natural frequency of the cavity,  $Q$  the figure of merit of the cavity, and  $Q_{\Lambda}$  the figure of merit of the spectral line.

It is seen from (1.1) that the smaller the width of the spectral line  $\Delta\nu = \nu_{\Lambda}/Q_{\Lambda}$ , the better the agreement between the maser frequency and the spectral-line frequency.

Formula (1.1), however, yields the maser frequency only accurate to  $10^{-8}$ . To obtain greater accuracy it is necessary to take into account many effects neglected in the model used in references 20-22.

In the derivation of (1.1) it was assumed that the transitions are between two energy levels, so that the emission line consists of a single component of definite frequency. The line usually used in the maser, that of the  $N^{14}H_3$  inversion spectrum,  $J=3, K=3$ , has a rich hyperfine structure, due to electric and magnetic interactions in the molecule.<sup>23</sup> The strongest of these is the electric quadrupole interaction between the nitrogen nucleus and the molecular field,<sup>24</sup> the coupling constant of which is 4 Mcs. The magnetic interactions are weaker, and the coupling constant is on the order of 25-100 kcs. These interactions include the spin-spin interaction between the hydrogen nuclei themselves, as well as the spin-spin interactions with the nitrogen nucleus and with the magnetic field of the rotating molecule.

The hyperfine interactions cause the lines of the ammonia conversion spectrum (including the line  $J = 3, K = 3$ ) to be split into several components corresponding to different quantum numbers  $I_H, I_N, K, F_1$ , and  $F$ ,\* which characterize the levels of the molecule with account of the hyperfine interactions.<sup>23</sup> Consequently, to describe the energy transition we must, strictly speaking, know not only the numbers  $J$  and  $K$ , but also the change in the numbers  $F_1$  and  $F$ .

The maser makes use of the most intensive components of the inversion transition  $J = 3, K = 3$ , which is diagonal in the quantum numbers  $F_1$  and  $F$ :  $\Delta F_1 = 0, \Delta F = 0$ . Were the coupling constants of the hyperfine interactions the same for the upper and lower inversion levels, the line  $\Delta F_1 = 0, \Delta F = 0$  would have only one component. As shown in reference 24, these constants differ for the upper and lower inversion levels, splitting the  $J = 3, K = 3$  and  $\Delta F_1 = 0, F = 0$  lines into twelve components corresponding to the twelve possible values of the quantum numbers  $F_1$  and  $F$  when  $J = 3$  (Fig. 3b). At the usual line widths, these components are not resolved and participate in the emission like a single spectral line. The position of the (frequency) peak of such a line depends on the relation between the intensities of the individual components and their frequencies. In the gaseous state, the intensities of the components are determined by the thermal distribution of the molecular energy levels. In a beam of sorted molecules, the relation between the component intensities changes, because the different components are differently sorted and the peak of the spectral line in the beam of the sorted molecules is shifted relative to the peak of the spectral line in gas.<sup>19,24</sup> This shift is not constant, but depends on the voltage on the sorting system,<sup>25</sup> since the relation between the intensities of the components changes with the voltage. In addition, different components have different dipole-moment matrix elements and saturation is reached at different fields in the cavity, bringing about a dependence of the maser frequency on the cavity field, i.e., in final analysis, a dependence on the intensity of the molecular beam.

A representation in which the cavity is replaced by an oscillating circuit with lumped parameters, as used in the derivation of (1.1), disregards the propagation of electromagnetic energy along the cavity. When a molecule travels through the cavity, it radiates in non-uniform fashion, since the probability of radiation depends on the time of stay of the molecule in the resonator. Owing to the unevenness in the radiation of the molecules, a wave is produced and carries along the cavity an energy that causes a Doppler frequency shift of the spectral line even when the resonator is operating in the  $E_{010}$  mode.<sup>21</sup> The magnitude and sign of this shift depend on the intensity of the

\* $F_1 = I_N + J, F = F_1 + I_H$ , where  $I_N$  is the spin vector of the nitrogen nucleus  $I_H$  is the total spin vector of the hydrogen nucleus, and  $J$  is the rotational momentum of the molecule.

beam of active molecules. At low beam intensity (weak saturation) the molecules radiate energy essentially when they leave the resonator, and consequently the flux of electromagnetic energy is directed opposite to the molecule velocity, decreasing the maser frequency. At high active-molecule beam intensity (large saturation), the radiation occurs predominantly during the first instants of the stay of the molecule in the cavity, and the energy flux has consequently the same direction as the molecules, thereby increasing the maser frequency. This shift in the maser frequency can be appreciably reduced by passing two identical but opposite beams through the cavity and drawing the power from the maser precisely at the midpoint of the cavity.<sup>21</sup>

As noted earlier, an important role is played in the maser by saturation, which contributes to the width of the observed spectral emission (or absorption) line. If the transit times of the molecules have a distribution  $\frac{1}{\tau} e^{-\tau/\bar{\tau}}$ , then the saturation factor  $a = d^2 E^2 / n^2$  and the square of the width  $\Delta\nu_{\text{trans}}$  of the spectral line, due to the transit time, enter into the expression for the square of the total line width in additive fashion

$$\Delta\nu_{\text{tot}} = \left[ (\Delta\nu_{\text{trans}})^2 + \frac{d^2 \beta^2}{\hbar^2} \right]^{1/2}. \quad (1.2)$$

In this case the maser frequency is independent of the saturation parameter. The real distribution of the molecule transit times in a sorted molecular beam differs from  $\frac{1}{\tau} e^{-\tau/\bar{\tau}}$  and depends on the voltage on the sorting system.<sup>25,26</sup> Such a line does not have a Lorentz shape, and the squares of the line widths due to the time and saturation enter into the expression for the square of the total width of the line in non-additive fashion. All these circumstances cause the effective width of the line, which enters into the expression for the maser frequency, to be dependent on the saturation parameter  $a$  or, what is the same, on the molecular beam intensity and on the voltage of the sorting system.

There are also other effects on which the maser frequency depends. Their influence however is much less than that of the effects mentioned above, and does not exceed  $10^{-11} \nu_\Lambda$ .

The maser frequency calculated with account of the foregoing effects<sup>26</sup> yields the following expression for  $\nu$ :

$$\nu = \nu_\Lambda \left[ 1 - \frac{\nu_\Lambda - \nu_0}{\nu_\Lambda} \frac{Q}{Q_\Lambda} G(U, a) + \Delta_1(U, a) + \Delta_2(U, a) \right]. \quad (1.3)$$

The function  $G(U, a)$  describes the dependence of the effective  $Q$  of the line on the voltage  $U$  of the sorting system and the intensity of the molecular beam (through the saturation parameter  $a$ );  $\Delta_1(U, a)$  and  $\Delta_2(U, a)$  are additive increments of the maser frequency, due to the presence of unresolved hyperfine

structure components and to the traveling-wave effect, respectively;  $Q_{\Lambda} = \nu_{\Lambda} l (kT/m)^{-1/2}$ ,  $l$  is the length of the cavity,  $m$  is the mass of the molecule,  $T$  is the temperature in the molecular-beam source, and  $\nu_{\Lambda}$  is the frequency of the inversion transition with the hyperfine structure neglected.

Reference 26 contains plots of  $G(U, a)$  and  $\Delta_1(U, a)$ . The frequency shift  $\Delta_2(U, a)$  due to the traveling-wave effect is calculated in references 21 and 27 for a multi-velocity molecular beam. The values  $\Delta_1$  and  $\Delta_2$  as functions of the sorting-system voltage and of the molecular-beam intensity can vary within a range  $5 \times 10^{-9} \nu_{\Lambda}$ . If  $\Delta_1 = \Delta_2 = 0$ , then the dependence of the maser frequency on the various parameters whose effects are incorporated in  $G(U, a)$  can be appreciably reduced by sufficiently accurate tuning of the cavity to the spectral-line frequency. It is quite difficult, however, to obtain high absolute frequency stability\* because of the strongly varying additive terms  $\Delta_1$  and  $\Delta_2$ , the influence of which on the maser frequency is sufficiently large and cannot be reduced by tuning the resonator frequency  $\nu_0$  to the spectral-line frequency  $\nu_{\Lambda}$ . To obtain highly stable masers it is therefore necessary to eliminate the traveling-wave effect and the influence of the hyperfine structure components. As noted earlier, the traveling wave effect can be greatly offset by using two identical opposite beams. The influence of the hfs components can be radically eliminated by using a line without a hyperfine structure.

The  $N^{14}H_3$  inversion transition line  $J = 3, K = 2$  and the  $N^{15}H_3$  inversion lines do not have a quadrupole hfs. The presence of magnetic components in these lines changes the maser frequency insignificantly, by less than  $10^{-11}$ . Consequently the foregoing lines can be successfully used to produce a maser of high stability.† In a maser<sup>26</sup> with two identical opposing molecular beams and using the  $N^{14}H_3$  line  $J = 3, K = 2$  for excitation, it was possible to obtain an absolute frequency stability  $10^{-10}$  by tuning the cavity to the spectral-line frequency through modulation of the pressure in the source of the molecular beam.

As reported in reference 27, a stability of the same order ( $10^{-10}$ ) can be obtained with a maser having only one beam (line  $J = 3, K = 2$ ). For this purpose it is necessary to determine accurately the maser parameters and compute a correction for the phase shift due to the traveling-wave effect.

The feasibility of sufficiently good maser frequency stability is essentially closely connected with tempera-

ture stabilization of the cavity. To obtain a relative frequency stability of  $10^{-11}$  over a long time (several hours) it is necessary to maintain the temperature of an invar\* cavity accurate to several hundredths of a degree; it is also necessary to stabilize the other oscillator parameters, such as the pressure in the beam source, voltage on the sorting system, etc., although if the cavity is accurately tuned to the spectral line the dependence of the maser frequency on these parameters is weaker than the dependence on the resonator temperature. Reports have been published of a generator<sup>28</sup> with a six-hour relative frequency stability of  $10^{-11}$ . In short time intervals, on the order of several seconds, when the generator parameters change but slightly, the change in frequency is  $10^{-13} - 10^{-14}$  (see reference 111).

Further increase in the maser frequency stability calls for narrow yet sufficiently intense spectral lines. In reference 29 it has been proposed that beams of slow molecules, i.e., molecules with mean velocity much less than the mean thermal velocity at room temperature, be used for this purpose. In the same reference methods are considered for obtaining slow-molecule beams and it is shown that with such beams an increase of the absolute stability of the maser frequency to  $10^{-12}$  becomes fully realistic.

A generator with rather high frequency stability, using a hydrogen-atom beam, has been recently constructed.<sup>101</sup> The initial line width of the induced radiation is approximately 1 cps. In this generator use was made of magnetic dipole transitions between the sublevels of the hyperfine structure of the ground state ( $1^2S_{1/2}$ ) of the hydrogen atoms.<sup>101</sup> The structure of the hydrogen atom levels and the change in the level energies in the magnetic field are illustrated in Fig. 4a.<sup>32</sup>

Until recently it seemed impossible to generate microwaves with atomic beams, owing to the smallness of the matrix element of the magnetic dipole moment. However, at a sufficiently long time of interaction between a beam of atoms sorted out by energies and the radiation field in the cavity, it becomes possible to satisfy the self-excitation conditions for the generator even in the case of a dipole magnetic interaction.

The time of interaction between the atoms and the radio-frequency field was increased by using an accumulating volume, as proposed by N. Ramsay.<sup>101-102</sup> He has shown that if a beam of atoms with polarized nuclei enters into a vessel whose walls have a suitable coating (for hydrogen atoms—a thin layer of paraffin), then the atoms can experience several thousand of reflections from the wall without a change in the nuclear momentum orientation. The atoms can remain in such a vessel as long as 1 sec, and if this vessel is placed

\*The absolute stability is determined by the accuracy with which one can tune the frequencies of two independent generators to the spectral line. The relative stability is determined by the accuracy with which the differential frequency of two oscillators is maintained over a definite time interval.

†A shortcoming of the  $N^{14}H_3$  3-2 line is the relatively low intensity. In generators of identical design the self-excitation coefficient is 10-12 times smaller for the 3-2 line than for the 3-3 line. By using  $N^{15}H_3$ , the stronger 3-3 line can be employed.

\*Somewhat better results can be obtained by using quartz resonators, a description of which can be found in reference 59.

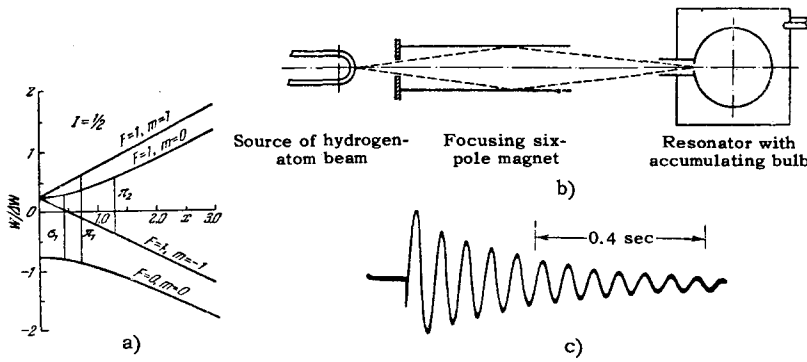


FIG. 4. a) Change in hyperfine structure sublevels in the magnetic field. b) Diagram showing arrangement of generator using hydrogen-atom beam. c) Attenuation of the beats of the induced radiation of the hydrogen-atom beam.

in a cavity tuned to the frequency of transition between the atomic energy sublevels, so long an interaction with the electromagnetic field can cause this system to operate as an oscillator.

The diagram of such an oscillator is shown in Fig. 4b. The hydrogen-atom beam from a Wood gas-discharge source<sup>32</sup> passes through a six-pole magnet, in which the atoms are sorted by energy states. The inhomogeneous field of such a magnet focuses the hydrogen-atom beam in states  $F = 1, m = 0$  and  $F = 1, m = 1$  on the entrance aperture of a quartz bulb, coated inside with a thin layer of high-melting-point paraffin. The bulb diameter is about 150 mm and its aperture 2 mm in diameter. This bulb is placed in a  $H_{011}$  cavity tuned to 1420.405 Mcs, corresponding to the transition  $F = 1, m = 0 \rightarrow F = 0, m = 0$ . If the vacuum is good enough, the atoms can have up to  $10^4$  collisions with the paraffin-coated walls without experiencing any strong disturbances, and then leave the bulb through the entrance aperture. The polarized atoms stay in the bulb about 0.3 sec. With a cavity  $Q$  of 60,000 and this value of the time, the minimum current needed for self excitation of the generator is  $4 \times 10^{12}$  atoms per second. The radiation power produced in the cavity in this case is  $10^{-12}$  watts. The output power of the generator is much smaller, owing to the weak coupling between the cavity and the radiation receiver. The width of the induced-emission line is 1 cps. The output signal of this generator is mixed with a 1450 Mcs signal from an "atomichron" and is amplified at an intermediate frequency 29.595 Mcs. After a second mixing with the frequency of a quartz oscillator and detection, this signal is observed on an oscilloscope.

If the generator self-excitation condition is not satisfied, then an additional signal applied to the cavity makes it possible to observe the induced emission of the hydrogen atoms. The self excitation condition was violated by reducing the time of stay of the atoms in the bulb (by increasing the diameter of the entrance aperture or reducing the intensity of the atomic beam) and also by reducing the  $Q$  of the cavity with more power drawn.

The added radio signal was applied in this case to the cavity from an external radio oscillator through a

second coupling loop, not shown in the figure. The maser operated in this case like a radiospectroscopy. If the auxiliary radio signal is applied to the under-excited maser in the form of a pulse of suitable power, then the atoms in the bulb continue to radiate after the termination of the pulse, and the induced emission can be observed on an oscilloscope (see Fig. 4c). The signal amplitude attenuated with a time constant of 0.4 sec, which is equal to the mean stay of the atoms in the bulb. This work was the first successful realization of the principle of accumulating volume, using the increased time of interaction between the particles and the radiation field, as proposed earlier by Dicke.<sup>38</sup> Such an oscillator and a spectroscopy can be used for many very precise physical researches. In particular, it can apparently be used to determine the hyperfine splitting for hydrogen isotopes with a considerably greater accuracy than hitherto possible.

When used as a time or frequency standard, such a maser will have much greater stability ( $10^{-12}$  and higher<sup>103</sup>) than any other previously proposed.

## 2. Cesium Frequency Standards

Cesium frequency standards are based on the use of a narrow line in the spectrum of a cesium atom beam.<sup>30-32</sup> The narrow line in the cesium atom beam does not excite oscillations in a cavity, as in the maser, but acts like a high- $Q$  frequency discriminator that stabilizes the frequency of a quartz oscillator. If the quartz oscillator has a high relative frequency stability, there is no need for continuously monitoring the latter; it is sufficient to introduce from time to time, with the aid of a cesium line, a correction for the oscillator frequency drift due to the "aging" of the quartz.

The arrangement of the cesium frequency standard is shown in Fig. 5.

A beam of cesium atoms passes through an inhomogeneous magnetic field. By virtue of the differences between the trajectories of the atoms in the various states, it is possible to obtain, using a diaphragm, a beam of atoms in a definite state. Usually the beam of atoms used for the frequency standard is in the state  $F = 4, m = 0$ .

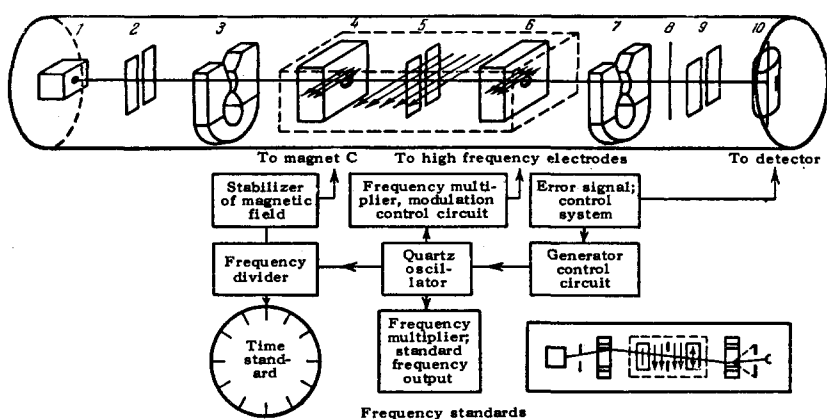


FIG. 5. Diagram of proposed arrangement of atomic clock.<sup>32</sup> 1 - Source; 2 - front slot; 3 - deflecting magnet A; 4 - high-frequency magnetic field; 5 - collimating slot; 6 - high-frequency magnetic field; 7 - deflecting magnet B; 8 - wire stop; 9 - image of slot; 10 - detector. Dimensions of tank: length 1.5 m, diameter 30.5 cm. Length of beam 1.22 m. The shading designates the region of constant magnetic field C. On the lower right is shown a top view of the instrument. The trajectory of the beam is shown and the focusing illustrated.

By passing this atomic beam through a cavity, and applying a high frequency field to the cavity, transitions are induced from the state  $F = 4, m = 0$  to the state  $F = 3, m = 0$ .

The frequency of this transition is  $\sim 9000$  Mcs (more accurately, 9192.632 Mcs).<sup>33</sup> After leaving the cavity, the beam again enters an inhomogeneous magnetic field, in which the atoms, now in the  $F = 3, m = 0$  state, are separated with the aid of diaphragms from the atoms remaining in the initial  $F = 4, m = 0$  state.

In experiments with molecular beams of alkali-metal atoms, high-sensitivity detectors based on surface ionization are used.<sup>32</sup> Therefore even when the molecular beam has low intensity ( $\sim 10^6$  atoms per second) it becomes possible to obtain indication with a large signal-to-noise ratio. The signal-to-noise ratio is determined by the residual gas in the vacuum bulb, and a detector with mass spectrometer and electron multiplier is therefore used to increase the sensitivity.

Resonance is indicated in two ways: a) the intensity of the atom beam of atoms that have passed into the  $F = 3, m = 0$  state is measured with the aid of a detector; b) a detector is used to register the reduction in the number of beam atoms in the initial  $F = 4, m = 0$  state. Since the transition probability increases with decreasing difference between the transition frequency and the frequency of the cavity field, the resonant frequency is fixed by the maximum number of atoms striking the detector in case a), or by the minimum number of striking atoms in case b). The accuracy in the determination of the resonant frequency depends on the width of the spectral line, and increases with narrowing of the line. The  $F = 4, m = 0 \rightarrow F = 3, m = 0$  transition is used because it is a "non-magnetic" transition, i.e., its frequency is almost independent of the external magnetic field, since the projection of the magnetic moment on the external field  $H$  is zero. However, a weak dependence still exists, so that<sup>33</sup>

$$\nu = (9192.632483 + 0,000427 H^2) \cdot 10^3 \text{ cps} \quad (1.4)$$

To obtain a narrow spectral line in a cesium frequency standard, the method proposed by Ramsay<sup>34</sup> is used, with two separate resonators (connected through a waveguide).

It is known that as  $\tau$  (the time of transit through the cavity) increases the line width  $\Delta\nu$  decreases:  $\Delta\nu = 1/2\pi\tau$ , but the inhomogeneity of the external magnetic fields increases at large transit distances, and since the frequency of the  $4, 0 \rightarrow 3, 0$  transition in cesium depends on the external magnetic field [see (1.4)], the increase in inhomogeneity of the external field with increasing resonator length increases the effective width of the line, in spite of the fact that the transit line width decreases. The use of two short separated cavities eliminates the line broadening due to the inhomogeneity of the magnetic field, since the inhomogeneity of the field in the space between the cavities does not play any role, for the molecules do not radiate when they travel between the cavities. At the same time, if the resonant radiation acting on the molecules that leave the first cavity has the same phase as at the entrance to the second cavity, the effective transit time is  $\tau_1 + \tau_0 + \tau_2$ , where  $\tau_1$  and  $\tau_2$  are the transit times in the first and second cavities respectively and  $\tau_0$  is the travel time between cavities.

If  $\tau_0$  is sufficiently long,\* then even when  $\tau_1$  and  $\tau_2$  are small it becomes possible to obtain a narrow spectral line ( $\sim 100$  cps) in this manner. Since the phase of the field in the coupled-cavity system depends on the frequency, the maximum of the observed line will depend on the phase difference between the cavity fields. This undesirable effect is eliminated by symmetrizing the observed spectral line, since the peak of a symmetrical line coincides with the frequency of the energy transition used in the apparatus.

A cesium standard<sup>35</sup> using two separated cavities has yielded an absolute frequency stability  $\pm 1.5 \times 10^{-10}$ .<sup>35</sup>

\*Installations in which the distance between cavities reaches 400 cm are now in existence.<sup>36</sup> Further increase in this distance is limited by the difficulty of obtaining well-focused and sufficiently intense atomic beams.



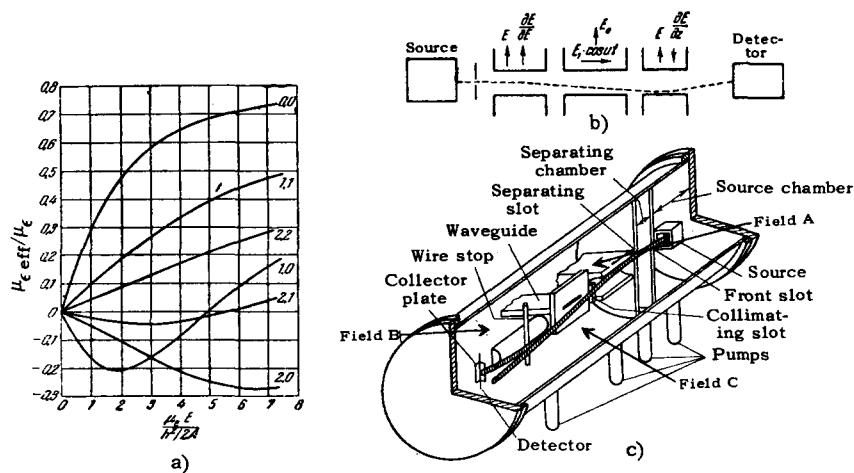


FIG. 6. a) Effective electric moments of a rotating polar linear molecule in an electric field (the interactions causing the hyperfine structure are neglected). b) Diagram of the electric-resonance method. c) Apparatus for electric-resonance study of a molecular beam.

The figures cited indicate that the absolute frequency stabilities of the cesium standard and maser standards are of the same order of magnitude. Further increase in the stability of the cesium frequency standard, as in the case of the maser, calls for the production of narrower spectral lines.

To narrow down the spectral line, Zacharias considered the possibility of slowing down cesium atoms in the earth's gravitational field.<sup>34,36</sup> However, this method does not yield a cesium-atom beam of sufficient intensity.

Ramsay proposed to increase the time of flight between cavities by having a beam of cesium atoms collide with a foreign gas or with the walls of a supplementary vessel placed between the cavities.<sup>37</sup> The collisions should be such as to lengthen the transit time between the cavities, but to leave the internal states of the cesium atoms practically unchanged. It is shown in reference 38 that such a foreign gas can be helium. The line width attainable in this manner is theoretically estimated<sup>39</sup> to be on the order of 1 cps. The procedure is apparently still in the development stage.\*

A certain gain in stability can also be obtained by replacing the cesium with thallium atoms,<sup>32</sup> where the transition frequency is higher ( $\sim 23,000$  Mcs), because high stability calls for a minimum ratio  $\Delta\nu_\Lambda/\nu_\Lambda$  (where  $\Delta\nu_\Lambda$  — width of the spectral line and  $\nu_\Lambda$  is its frequency), so that a beam of thallium atoms yields a higher line Q for the same distance between the cavities. In addition, thallium is somewhat heavier than the cesium, so that its thermal velocity in the beam is decreased and the transit time  $\tau$  increased. There have been no reports, however, of realization of these advantages of thallium, apparently because thallium beams are more difficult to sort than cesium beams.

\*A cesium standard (apparently employing the aforementioned principle) has been reported<sup>110</sup> to yield a frequency stability  $\pm 2 \times 10^{-12}$  over nine months.

### 3. Other Frequency Standards

It is also possible to build a molecular-beam frequency standard using rotational spectral lines. This method, called the electric resonance method,<sup>32,40,41,42</sup> employs a procedure similar to that of the magnetic-resonance method used in the cesium frequency standard (see reference 1, Sec. 2).

In view of considerable electric dipole moments of the molecules, it is possible to sort a beam of such molecules with an inhomogeneous electric field. Figure 6a shows the dependence of the dipole moments of diatomic molecules on the field and on the states of the molecules ( $J, M_j$ ). The apparatus for the observation of electric resonance<sup>41</sup> (Fig. 6b) employs a molecular beam, which is deflected by inhomogeneous electric fields in tandem, between which are located a constant homogeneous electric field and cavities in which is produced the high frequency electric field that causes the transitions between the rotational energy levels of the molecules in the beam. The change in intensity of the beam is detected as in the magnetic resonance.

In reference 42 are given the results of research on alkali metal halide molecules, particularly  $\text{Li}^6\text{F}^{19}$  [the transition between the rotational energy levels  $J = 0 \rightarrow J = 1$  corresponds to an emission frequency of about  $10^{11}$  cps ( $\lambda \sim 3$  mm)]. Other molecules can also be used,<sup>43</sup> but molecules containing alkali-metal atoms are preferable, since very sensitive detectors are available for beams of such molecules.<sup>32,40</sup>

The expected stability of the frequency standard in the electric resonance method<sup>42</sup> is on the order of  $10^{-10}$ , that is, the same as in the cesium frequency standard.

Recently developed frequency standards are based on detection of the microwave absorption at the spectral lines of monatomic alkali-metal vapors with the aid of atomic transitions in the optical or infrared bands.<sup>44-48,58</sup> This method of detection has very high sensitivity, because photomultipliers with very low noise level can be used to detect the optical or

infrared transitions. In many papers it is also proposed to use auxiliary infrared or optical radiation to obtain a negative temperature in alkali-metal vapor.<sup>107-109</sup> Such negative-temperature systems can be used to produce masers. By diluting alkali-metal vapor in an inert gas that induces no level transitions in the alkali-metal atoms on collision, sufficiently narrow spectral lines are obtainable, since the Doppler broadening of the spectral line is determined in this case not by the thermal velocity of the radiating atoms, but by the rate of their diffusion in the inert gas.<sup>38</sup>

We describe briefly the use of the ground-state transition  $F = 2 \rightarrow F = 1$  in sodium vapor, corresponding to a frequency of 1772 Mcs ( $\lambda \sim 17$  cm) (Fig. 7).

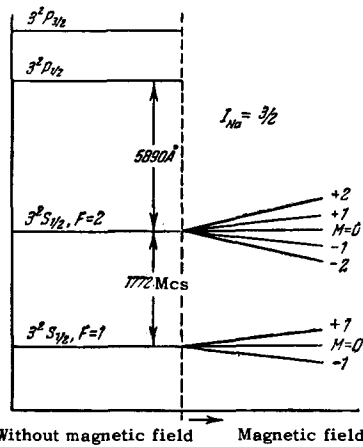


FIG. 7. Level scheme of sodium atoms.

The apparatus<sup>46</sup> employs the "non-magnetic" transitions  $F = 2, m = 0 \rightarrow F = 1, m = 0$ ; a diagram of the apparatus is shown in Fig. 8. An absorbing cell of quartz, filled with low-pressure sodium vapor mixed with argon, which serves as a buffer gas, is placed in an evacuated cylindrical cavity with  $Q \sim 10,000$ . At a cell temperature of  $\sim 135^\circ \text{C}$ , the sodium vapor pressure is  $\sim 10^{-5}$  mm Hg and the argon pressure is  $\sim 100$  mm Hg. Light from a sodium lamp, which excites the sodium atoms in the absorbing cell and causes a difference in the energy-level populations ("optical pumping"), is applied to the absorbing cell through filters and windows in the cavity. The cavity operates in the  $H_{011}$  mode at a resonant frequency  $\sim 1772$  Mcs, corresponding to the frequency of the  $F = 2 \rightarrow F = 1$  transition, excited by a frequency-modulated oscillator with low depth of modulation. The receiver comprises a photomultiplier and a phase detector. The signal from this apparatus, an oscillogram of which is shown in Fig. 9, is used to regulate the frequency of a radio-frequency oscillator. The frequency stability obtained with such a device is about  $10^{-8}$  and can be improved by perfecting the instrument. The main advantage of frequency standards of this type are simplicity and low weight compared with other types (particularly compared with the cesium standard).

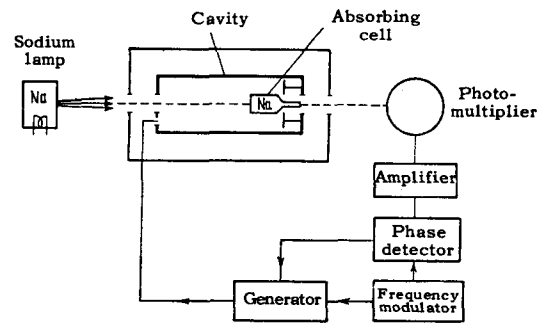


FIG. 8. Diagram of frequency standard with "optical pumping."

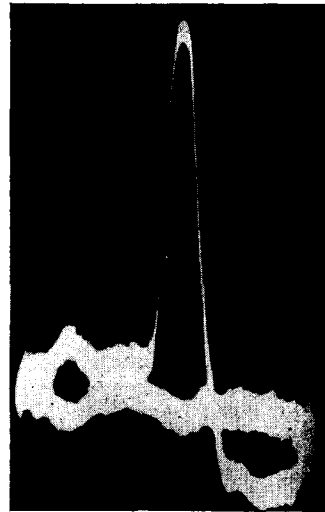


FIG. 9. Oscillogram obtained from an optical-resonance detector

One of the first high-accuracy frequency standards is an oscillator stabilized with a quartz resonator. Quartz standards have by now reached a very high relative frequency stability,<sup>49</sup> on the order of  $10^{-10}$  (even  $10^{-11}$  if the quartz resonator is placed in liquid helium). Quartz generators are by their nature secondary standards, and the frequency of each generator must be calibrated; it is impossible to prescribe a procedure for preparing a quartz standard that would yield oscillators of a prescribed frequency, unlike molecular and atomic standards, which operate near the natural frequency of the spectral line.

References 49 and 50 give the results obtained with high-accuracy quartz generators and compare their frequency stability with that of masers and cesium standards.

These results show that quartz resonators with  $Q$  on the order of  $10^8$ , immersed in liquid helium, are exceedingly stable. The frequency deviation is small ( $\sim 10^{-11}$ ) and has a monotonic drift (Fig. 10); this drift can be greatly reduced by regulating the gas pressure over the liquid helium, but at the cost of a slight reduction in the short-time stability. The stability of the better quartz generators at ordinary tem-

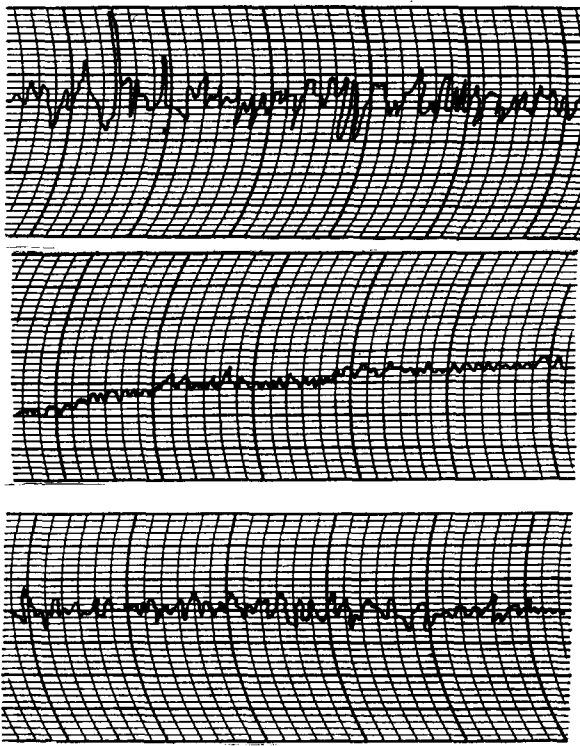


FIG. 10. Time variation of quartz-generator frequency.

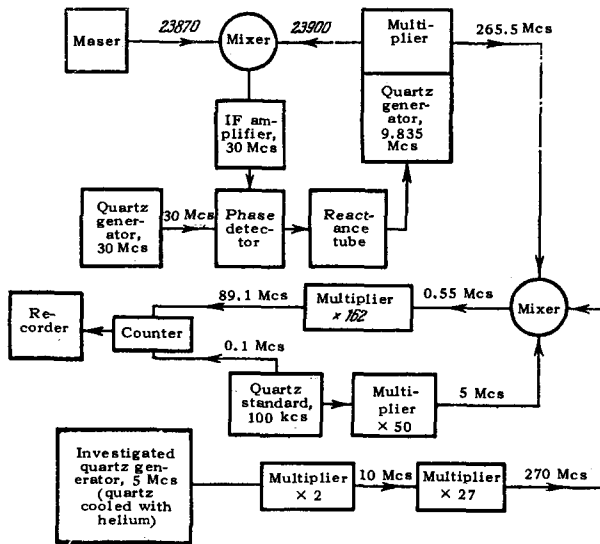


FIG. 11. Measurement of the stability of quartz generator.

peratures, if good thermostats are used to maintain the cavity temperature accurate to  $10^{-4} - 10^{-3}$  deg, is also quite high and reaches several times  $10^{-10}$ . A circuit for the measurement of frequency stability<sup>50</sup> is shown in Fig. 11.

4. Frequency Stabilization

Though highly stable, a maser has exceedingly low output power, on the order of  $10^{-11} - 10^{-10}$  watts, insufficient for many experiments and applications. To

obtain sufficient power it is necessary either to amplify the maser oscillations, or to tune and synchronize more powerful generators (say klystron generators) with the maser. In either case more powerful generators with the high frequency stability possessed by the maser are obtained.

A low-noise amplifier (such as a traveling wave tube) followed by an amplifying klystron must be used (direct klystron amplification is impossible owing to the high internal noise of the klystron). Amplification with a travelling-wave tube or a parametric amplifier leads to instability of the phase of the amplified signal, so that automatic phase control must be used for phase measurements of high accuracy.<sup>52</sup> Automatic phase control (APC) of a klystron using a maser was first proposed by Strendberg.<sup>51</sup>

APC circuits were subsequently improved by various researchers.<sup>53,54,56</sup> Automatic frequency control was also obtained.

In the initial variant, the klystron was tuned directly to the maser; this circuit had several major shortcomings, the most important being the narrow bandwidth of permissible klystron-frequency deviations from the set value (narrow "locking" and "holding" band), and the possibility of the locking of the maser frequency by the more powerful klystron.

To improve the circuit, an auxiliary (reference) quartz oscillator was introduced, and the amplification was at an intermediate frequency (Fig. 12); although this reduced the possibility of locking the molecular generator frequency, it nevertheless did not exclude it, particularly at considerable klystron power (more than 10 milliwatts). The stability of the reference generator must also be sufficiently high.

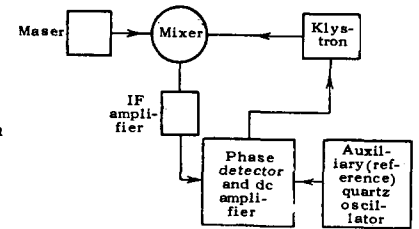


FIG. 12. Automatic phase control (APC) of a klystron frequency with a maser.<sup>51</sup>

Later improved circuits with subtraction of the reference-generator error were developed,<sup>54</sup> as well as a klystron APC using the mean frequency of two ammonia lines. In the latter case the reference generator used was a dual maser with cavities tuned to the  $N^{14}H_3$  lines  $J = 3, K = 3, f = 23,870.13$  Mcs and  $J = 2, K = 2, f = 23,722.61$  Mcs (Fig. 13); since the klystron frequency differed greatly from the frequencies of the two masers and was not a multiple of these frequencies, the possibility of locking the maser frequency was practically eliminated even at high klystron power.

In direct APC of a klystron with a maser, a "locking" band of  $\pm 100$  kcs was obtained, but since the frequency stability on ordinary klystrons is less than

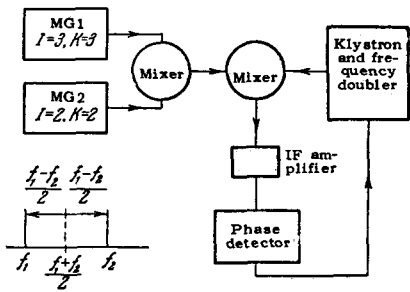


FIG. 13. Automatic phase control of a klystron using the mean frequency of two masers.<sup>113</sup>

$10^{-5}$ , it must first be stabilized with a quartz generator. In this case the overall locking band is  $\pm 2.5$  Mcs. The required stability of the quartz generator is low, and the circuit is sufficiently simple and reliable.

If the klystron has relatively high frequency stability, the need for preliminary synchronization against a quartz generator is obviated.

Thus, automatic phase control of a klystron using the mean frequency of two molecular generators has the following advantages:

1. The circuit permits amplification of the power from weak masers at an intermediate frequency of 73 Mcs.
2. The circuit does not require a stable auxiliary reference generator.
3. Possible frequency locking of the maser by the klystron is eliminated even if the klystron is sufficiently powerful.

In the case when not more than several milliwatts are to be delivered by the klystron, the circuit with subtraction of the reference-generator error<sup>54</sup> is perfectly suitable (Fig. 14).

In the improved version of the two-klystrons circuit with error subtraction<sup>55</sup> (Fig. 15), three frequency outputs are possible:  $f_0/k$  in the centimeter band ( $k = 1, 2, 3$ ),  $f_0/km$  in the decimeter band ( $m = 3-10$ ), and  $f_0/kmn$  in the meter band. The following relations between frequencies are used:

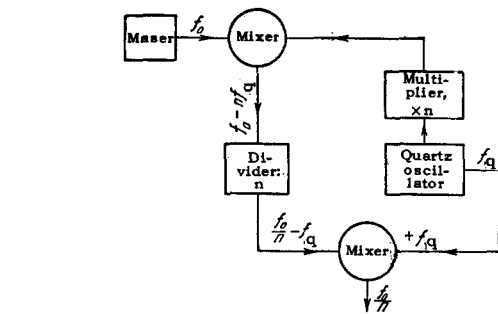
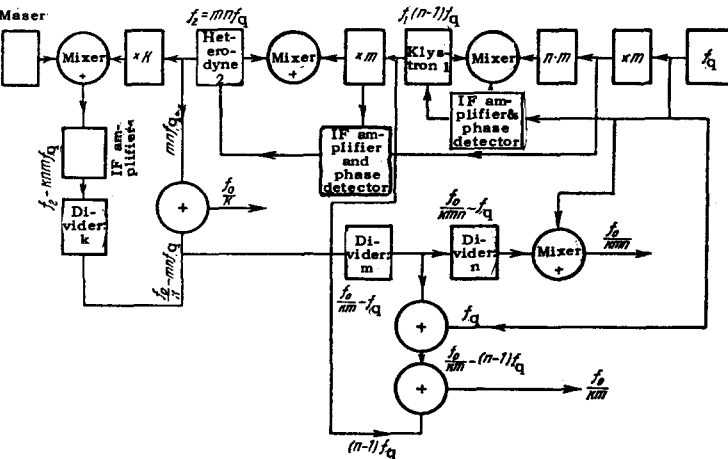


FIG. 14. Block diagram of automatic phase control of klystron frequency using a maser with subtraction of the error of the auxiliary reference generator.<sup>54</sup>

$$f_1 = (n-1)f_q,$$

$$f_2 = mf_1 - mf_q = (mn - m + m)f_q = mnf_q,$$

$$f_{if} = f_0 - kmnf_q,$$

where  $f_1$  — frequency of the first klystron,  $f_2$  — frequency of second klystron,  $f_q$  — frequency of quartz generator,  $f_0$  — frequency of molecular generator, and  $f_{if}$  — intermediate frequency.

The subtraction of error is based on frequencies  $f_2$ ,  $f_1$ , and  $f_q$ :

- 1) Subtraction based on  $f_2$ :

$$\frac{f_0 - kmnf_q}{k} - f_2 = \frac{f_0}{k} - mnf_q + mnf_q = \frac{f_0}{k}.$$

- 2) Subtraction based on  $f_1$ :

$$\frac{f_0 - kmnf_q}{km} - f_1 + f_q = \frac{f_0}{km}.$$

- 3) Subtraction based on  $f_q$ :

$$\frac{f_0 - kmnf_q}{km} + f_q = \frac{f_0}{kmn}.$$

This improved circuit has a broader locking band than with the APC circuit using the mean frequency of the two masers but likewise does not exclude the possibility of locking.

As noted earlier, along with using automatic klystron frequency control, it is also possible to amplify the output of the maser directly. The overall gain necessary

FIG. 15. Improved APC circuit with subtraction of error of the reference generator.<sup>55</sup>

to obtain an output of several times 10 milliwatts should be about 90 db, with pre-amplification on the order of 30 db by means of a traveling-wave tube. The use of parametric amplifiers or traveling wave tubes leads to phase fluctuations of the amplified signal, so that it is impossible to employ the amplified signal in phase-measurement circuits. Better results are obtained with quantum paramagnetic amplifiers, but slight phase oscillations still remain.

It is also possible to use a traveling-wave tube or a klystron to divide the frequency of the amplified maser signal.

## II. USE OF HIGHLY STABLE FREQUENCY AND TIME STANDARDS TO CHECK GENERAL AND SPECIAL RELATIVITY

### 1. Possible Experiments to Check General Relativity

The now feasible high absolute frequency stability of the maser, on the order of  $10^{-10}$  (see Ch. I), enables us to set up experiments to check the general theory of relativity (theory of gravitational field). There are three widely known effects that follow from general relativity and admit of experimental verification.<sup>60,61,62,63</sup> These are the relativistic shift of the perihelion of Mercury, the deflection of light beams by the sun's gravitational field, and the relativistic red shift of the spectral lines of the light from the sun and from several stars. The last effect was observed also in the earth's gravitational field, using narrow gamma-ray spectral lines, emitted and absorbed by radioactive nuclei in crystals cooled to liquid helium temperature<sup>64</sup> (Mössbauer effect<sup>2</sup>). All three effects have very small absolute magnitudes, and their experimental verification entails great difficulties.

In the last decade all three Einstein effects along with methods for their experimental verification and the accuracy of the results obtained, have been extensively discussed in the literature. Other effects, which follow from general relativity, were also considered.<sup>65,66,67</sup> Attempts have been made to observe experimentally some of these, such as cosmic gravitational waves.<sup>68</sup> We shall discuss briefly only three effects.

According to general relativity, the elliptic orbit of a planet rotates around the sun in the plane of the orbit in the same direction as the moving planet. For Mercury,<sup>69</sup> this rotation (relativistic shift of the perihelion) should amount to  $43.03 \pm 0.03$  seconds of angle per century. The actually observed shift of the Mercury perihelion amounted to  $5509.79'' \pm 0.41''$  per century. A shift amounting to  $5557.18'' \pm 0.85''$  minutes is accounted for by classical theory (the perturbing action of other planets, precession, etc.). The difference,  $42.56'' \pm 0.94''$ , remained unexplained until the formulation of the general theory of relativity, but is

within the experimental error inherent in the theoretical prediction. If this difference were much greater than the overall measurement error, the results could be regarded as a good experimental check on the general relativity theory. For the earth,<sup>70</sup> the actually observed shift of the perihelion is  $6183.7'' \pm 1.1''$  per century. Of this amount, only  $4.6'' \pm 2.7''$  is due to the relativistic effect, which theoretically should be  $3.8'' \pm 0.0''$ . The observed results and the theory thus agree within the limits of experimental error, in this case, too, but the fact that the relativistic shift is somewhat greater than the measurement error does not enable us to regard it as a reliable confirmation of the theory. For other planets or the moon, the relativistic shift of the perihelion is negligibly small and was never observed.

The second effect calls for the light rays coming from the stars to the earth and passing near the sun's surface to be bent toward the sun's center by  $1.75''$ , as would follow from general relativity calculations. Photography of the placement of the stars around the sun's disc during a total eclipse, followed by photography of the same stars in the same place in the absence of the sun, enables us to measure the deflection. The mean value of the angle, as measured by three expeditions during the eclipses of 1919 and 1922, proved to be  $1.79'' \pm 0.30''$ , in good confirmation of the theory.<sup>60</sup>

The principle of equivalence of the inertial and gravitational masses, which is the basis of the general theory of relativity, determines the relativistic red shift of the spectral lines of light radiated from the sun and from the stars (see the Appendix). Since they possess mass, the photons radiated from the surface of a star should overcome on their path to the earth the force of attraction to the star, performing work against this force. The photon energy and thus its frequency should therefore decrease and the spectral line should shift toward the red end of the visible spectrum. On the sun's surface this shift should be  $2.12 \times 10^{-6}$  of the frequency of the spectral line.<sup>60</sup> Observations have disclosed such a shift only up to the edges of the sun's disc, the shift being considerably smaller for the remainder of the sun's disc.<sup>71</sup> The relativistic red shift for the white dwarf Sirius B is several dozens of times greater than that for the sun, but it follows from the observations that it is approximately three times smaller from that predicted by the general relativity theory.<sup>71</sup>

These experiments prove the existence of a relativistic red shift, but the absence of a quantitative agreement with the theoretical predictions is attributed to the influence of other factors, comparable in magnitude with the observed effect. Such factors are the fast rising currents in the sun's atmosphere and the inexact knowledge of the radius of Sirius B.

The fundamental character of the general theory of relativity does not enable us to regard the hitherto ob-

tained confirmation of its deductions as sufficient, and new efforts toward an experimental verification of the theory are urgently needed. The mentioned experiment of Pound and Rebka<sup>64</sup> made it possible to measure the relativistic shift of the gamma-ray frequency in the earth's gravitational field accurate to 4 percent. The measured value of this shift agreed with that calculated from the general theory of relativity.<sup>1</sup> The launching of artificial satellites and the development of highly stable masers afford a new possibility of such verification.<sup>4,6,65,72-78</sup> If two identical masers have equal frequencies over a prolonged time of operation, with accuracy on the order of  $10^{-10} - 10^{-11}$ , and one is placed on a satellite while the other is left on earth, the frequency of the former, measured on the satellite, and that of the latter, measured on the earth, will again be equal to each other within the accuracy limits indicated above. However, the frequency of the maser placed on the satellite, and measured by an observer situated on earth, will change as a result of the first and second order Doppler effects and as a result of the gravitational frequency shift. It will be shown below that for a satellite the combined action of the second-order Doppler effect and the gravitational effects can cause a relative frequency change of the order of  $10^{-9}$ , whereas the first-order effect can change the frequency by an amount on the order of  $10^{-4} - 10^{-5}$ . Therefore to measure the gravitational frequency shift it is necessary first to exclude the first-order Doppler effect.

For this purpose, it has been proposed<sup>4</sup> to measure accurately long time intervals on the earth and on the satellite and subsequently compare these intervals by radio communication. The gist of the method is as follows. A highly stable master oscillator (say, a maser) is placed on the satellite, together with a scaler device that generates short electric pulses spaced a definite number of maser cycles apart. These pulses are transmitted to the earth and are recorded simultaneously with similar pulses produced by identical land-based apparatus. After a prolonged recording session (not necessarily continuous), a difference arises in the duration of the long time intervals elapsed on earth and on the satellite between pairs of corresponding pulses obtained from the earth and from the satellite.

According to relativity theory, this time difference is due to the gravitational field and to the second-order Doppler effect.

If the satellite moves in a circular orbit around the earth, then the frequency shift due to the foregoing causes will be constant and the difference in the time intervals will therefore be<sup>4</sup>

$$\Delta \equiv \frac{dt_{\text{sat}} - dt_{\text{ear}}}{dt_{\text{ear}}} \approx 7 \cdot 10^{-10} \left( \frac{1.5}{1 + \frac{h}{r}} - 1 \right), \quad (2.1)$$

where  $dt_{\text{sat}}$  — time interval elapsed on the satellite,  $dt_{\text{ear}}$  — the corresponding time interval elapsed on earth,  $h$  — height of satellite above the earth, and

$r$  — radius of the earth. Since the absolute value of  $\Delta$  does not exceed  $7 \times 10^{-10}$ , the time intervals must be measured with accuracy on the order of  $10^{-11}$ . If  $dt \approx 10^4$  sec, the pulse duration should be about 0.1 microsecond. Within that time the radio waves travel approximately 30 m, and consequently to introduce corrections for the time of propagation of the radio signals from the satellite to the earth it is necessary to know exactly the coordinates of the satellite position, so as to determine the distance from the satellite at any very accurately specified instant of time. At the same time it is necessary to maintain the master oscillators on earth and on the satellite very stable during the prolonged time of operation, with stability on the order of  $10^{-11}$  over several hours or days. In any case, such stability is required for the mean frequency of the master oscillators, if the deviations from this mean frequency are random and have a normal distribution (no frequency drift). Then the necessary measurement precision is obtained by averaging over the time. For example, if the frequency is  $10^{10}$  cps with a mean-square deviation  $\pm 10$  cps (frequency stability  $10^{-9}$ ), and if the measured frequency shift is 1 cps ( $\Delta = 10^{-10}$ ), then after  $10^4$  seconds the measured shift amounts to 10,000 cycles, whereas the measurement error, which increases as the square root of the time, will be  $\pm 1,000$  cycles. The accuracy in the measurement of the time intervals will then reach  $10^{-11}$ . In this experiment, any constant frequency shift between the master oscillators, due to any cause, cannot be separated from the gravitational shift and from the second-order Doppler effect. These circumstances make such an experiment difficult.

Another method of eliminating the first-order Doppler effect was proposed in reference 5. To simplify the formulas and clarify the derivation, it is proposed that the point of observation be at an earth pole, the point O on Fig. 16. A signal of frequency  $f$ , stabilized with a maser, is transmitted from there toward the satellite. According to relativity theory, the frequency of the signal received and measured on the satellite is<sup>61,63</sup>

$$f' = f \frac{1 - \beta \cos \alpha}{\sqrt{1 - \beta^2 + 2\Phi}}. \quad (2.2)$$

Here  $\beta = v/c$ , where  $v$  is the velocity of the satellite at the instant of signal reception and  $c$  is the velocity of light,  $\alpha$  is the angle between the radius from the point O to the satellite and the satellite velocity vector, measured in a coordinate frame fixed to the observer at the point O at the instant when the signal is received on the satellite, and  $\Phi$  is the (positive) difference in the gravitational potentials of the earth between the points O and S, divided by the square of the velocity of light. The satellite carries an oscillator of frequency  $2f$ , as measured on the satellite; this frequency is stabilized with a maser on the satellite. The frequency  $f'$  of the received signal is mixed on the

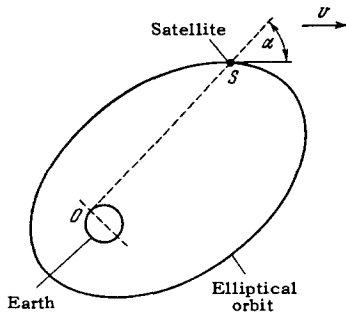


FIG. 16. Space relationships in an experiment with an artificial satellite.

satellite with the frequency  $2f$ , and the difference-frequency signal

$$f'' = 2f - f' \tag{2.3}$$

is radiated from the satellite to the observer on earth. It is assumed that the delay time on the satellite between the instant when the signal is received from the earth and retransmitted to the earth is negligibly small. The signal received on the earth from the satellite will have a frequency

$$f''' = f'' \frac{\sqrt{1 - \beta^2 + 2\Phi}}{1 + \beta \cos \alpha} \tag{2.4}$$

This formula is the inverse of the formula (2.2) for  $f'$ . Substituting (2.2) and (2.3) in (2.4), expanding the result in powers of  $\beta$  and  $\Phi$ , retaining the terms quadratic in  $\beta$  and linear in  $\Phi$ , and discarding all the higher powers of these quantities and of their products, we obtain

$$f''' = f(1 + 2\Phi - \beta^2). \tag{2.5}$$

Thus, the frequency of the signal received on earth will differ from the frequency of the signal received from the earth by an amount

$$\Delta f = f''' - f = f(2\Phi - \beta^2). \tag{2.6}$$

This difference does not contain the frequency shift due to the first-order Doppler effect ( $-\beta \cos \alpha$ ), and comprises the gravitational shift ( $+\Phi$ ) and the shift due to the second-order Doppler effect ( $-\beta^2/2$ ). The results obtained can be illustratively interpreted as follows. The frequencies of the signals radiated from the earth and from the satellite are practically equal to each other, and therefore their first-order Doppler shifts will be approximately equal in magnitude and in time. But the frequency of the signal transmitted from the satellite already contains a first-order Doppler shift of the same magnitude but of opposite sign, since according to (2.3) any shift in the frequency of the signal received on the satellite causes a shift of similar magnitude but of opposite sign in the frequency of the signal radiated by the satellite. Therefore the frequency of the signal received on earth will be shifted twice by the same amount, but in opposite directions, so that the first-order Doppler effect cancels out. For the same reason, the difference (2.6) contains double the frequency

shift due to the gravitational effect and the second-order Doppler effect. Indeed, the frequencies of the signals from the earth and from the satellite will have gravitational shifts of the same magnitude but of opposite sign, since in the former case the radio-wave energy quanta will work against the earth's gravitation, causing a reduction in the signal frequency, while in the latter the quantum energy will be increased by the potential energy of the earth's gravitational field, so that the signal frequency will increase. Since according to (2.3) the frequency of the signal radiated from the satellite is already increased by the gravitational shift, the frequency of the signal received on earth will contain double the gravitational shift, which can be called the violet shift (analogous to the gravitational red shift of the spectral lines of light), since it increases the frequency. The second-order Doppler effect is thus doubled and leads to a decrease in the frequency of the signal received on earth (red shift).

Actually the cancellation of the first-order Doppler effect will be incomplete, primarily because (2.5) is approximate of order not higher than the second in  $\beta$ . Of only importance to the experiment is that the uncompensated part of the first-order Doppler effect not exceed the permissible measurement error, which for further qualitative estimates can be assumed to be  $10^{-11}$ . An account of the terms cubic in  $\beta$  will cause the right half of (2.6) to be multiplied by another factor  $(1 - \beta \cos \alpha)$ . For the actual velocities and positions of the satellite relative to the earth, these terms are on the order of  $10^{-14}$ , and this determines the accuracy of (2.6).

Another important factor in the cancellation of the first-order Doppler effect is the time elapsed between the instant when the earth signal is received on the satellite and the instant of retransmission to the earth, a time assumed negligibly small in the derivation of (2.6). During that time, the radial velocity of the satellite relative to the land-based observer (the rate of change of the distance between the satellite and the observer), changes and consequently the frequency shift due to the first-order Doppler effect in the signals received on the satellite will differ from that of the signal transmitted from the satellite. This difference determines the uncompensated part of this effect. Assume, for example, that the signal time delay on the satellite is  $\Delta t = 10 \mu\text{sec}$ . The acceleration of a satellite moving in the earth's gravitational field does not exceed  $g = 1000 \text{ cm/sec}^2$ ; the radial velocity therefore changes during the delay time by less than  $\Delta v = g\Delta t = 0.01 \text{ cm/sec}$ . The uncompensated part of the first-order Doppler effect, which is the ratio of the change in the radial velocity to the velocity of light, will be less than  $\Delta v/c = 3 \times 10^{-13}$ .

In another case, the disturbance to the compensation can be greater. If the satellite moves horizontally above the observer with constant velocity  $v = 10$

km/sec at a height  $h = 300$  km (Fig. 17), then its radial velocity is  $v \sin z$ , where  $z$  is the zenith distance of the satellite. In a time interval  $\Delta t = 10^{-5}$  sec this velocity changes by  $\Delta v = v \frac{d \sin z}{dt} \Delta t$ . But \*

$$\frac{d \sin z}{dt} = \cos^3 z \frac{d \tan z}{dt} = \frac{v}{h} \cos^3 z$$

and has a maximum when  $z = 0$ . Then

$$(\Delta v)_{\max} = \frac{v^2 \Delta t}{h} \approx 0.3 \text{ cm/sec}$$

and the uncompensated part of the first-order Doppler effect will reach  $(\Delta v)_{\max}/c \approx 10^{-11}$ , a value equal to the permissible measurement error.

If no special delay lines are used in the satellite apparatus, the actual value of the delay time of the signal on the satellite is of the same order as the reciprocal of the bandwidth of the receiver.

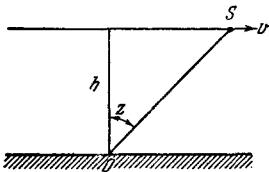


FIG. 17. Satellite above the point of observation on earth.

The compensation of the first-order Doppler effect will also be disturbed if the frequencies of the master oscillators on earth and on the satellite are not the same, so that a signal of frequency  $f$  radiated from the earth is mixed on the satellite with a frequency  $2f_1$ , where  $f \neq f_1$ . Then the right half of (2.6) will be supplemented by two terms  $2(f_1 - f) + (f - f_1)2\beta \cos \alpha$ , of which the first is the uncompensated part of the first-order Doppler effect. At a satellite radial velocity of approximately 7 km/sec, the uncompensated part will be less than the permissible measurement error ( $10^{-11}$ ) if

$$|f - f_1| < 2 \cdot 10^{-7} f. \quad (2.7)$$

The term  $2(f_1 - f)$  is a constant frequency shift, independent of the velocity of the satellite and of the earth's gravitational potential near the satellite. If condition (2.7) is satisfied, this term can appreciably exceed the right half of (2.6). Consequently, to separate the gravitational frequency shift and the second-order Doppler effect from the total frequency shift, it is necessary to use the dependence of the terms in the right half of (2.6) on the satellite velocity and on the earth's gravitational field. It will be shown below that when the satellite moves in an elliptical orbit, the quantities in the right half of (2.6) vary periodically with time, the period being equal to that of the satellite about the earth. This is a method of measuring (2.6) by determining the "modulation" amplitude. It is simultaneously possible to measure, with the same accuracy, the frequency difference  $f_1 - f$ ; the sign of this

\* $\tan z = \frac{v}{h}$ .

difference can be readily determined from its variation resulting from a small change in the frequency  $f$  of the earth-based maser or from the form and phase of the dependence of the total registered frequency difference  $2(f_1 - f) + f_1(2\Phi - \beta^2)$  on the position of the satellite in its orbit.

Thus, the described method of eliminating the first-order Doppler effect in two-way radio communication with the satellite is at the same time a method of measuring on earth the frequency of the satellite-borne maser, with the same accuracy with which the frequency of the earth-based maser is known.

This circumstance permits in turn an exact measurement of the radial velocity  $v_r$  of the satellite relative to the earth-based observer, using the first-order Doppler effect, by transmitting an additional signal of frequency  $f_0$  stabilized by a satellite-borne maser from the satellite to the earth. If the frequency difference  $f_1 - f$  is measured accurate to  $\pm 10^{-11} f$ , then the simultaneously measured Doppler shift of the frequency  $f_0$ , equal to  $f_0' - f_0 = -f_0 \beta \cos \alpha = -v_r f_0 / c$ , can also be determined accurate to  $\pm 10^{-11} f_0$ . The error  $d(v_r)$  in the radial velocity is connected with the error  $d(f_0' - f_0) = 10^{-11} f_0$  in the Doppler shift of  $f_0$  and with the error  $d(f_0)$  in the absolute value of  $f_0$  by the relation

$$\frac{d(v_r)}{c} = \frac{d(f_0' - f_0)}{f_0} + \frac{v_r}{c} \frac{d(f_0)}{f_0}.$$

The first term in the right half of this equation has an order of  $10^{-11}$ . The second term is smaller than  $10^{-12}$ , since the radial velocity of the satellite cannot exceed the sum of the second cosmic velocity (11.2 km/sec) and the linear velocity of the earth's rotation on the equator ( $\sim 0.5$  km/sec) if  $d(f_0) \leq 2 \times 10^{-8} f_0$ . In this case the error in the measurement of the radial velocity of the satellite will be

$$d(v_r) \approx 10^{-11} c = 0.3 \text{ cm/sec.}$$

There is no particular difficulty in determining the absolute maser frequency within  $10^{-8}$ .

To facilitate the measurement of the gravitational frequency shift conditions should be chosen such that  $2(f_1 - f)$  is of the same order of magnitude or less than  $f_1(2\Phi - \beta^2)$ . This can be accomplished by slight adjustment of the frequency of the earth-based maser.\*

If the radio communication between the observer and the satellite is at 500 Mcs, the difference (2.6) can reach 0.5 cps. By recording this difference at the observation point and by measuring the total change in phase over a period of ten seconds, with accuracy  $\pm 36^\circ$ , it becomes possible to measure<sup>5</sup> the difference (2.6) within  $\pm 0.01$  cps.

The short time needed for a single measurement (less than one minute) offers great practical advan-

\*To simplify the formulas we assume that  $f$  and  $f_1$  are equal, unless otherwise stipulated.



tages. Measurements made at different satellite positions on its elliptical orbit make it possible to separate the changes in the difference (2.6) having the same period as the satellite orbit from the small frequency drift of the masers. This will increase the measurement accuracy to an extent that quartz oscillators may become feasible in lieu of masers.<sup>5,80</sup> For greater measurement accuracy it will be necessary to stabilize the quartz oscillators with masers.

The two terms in (2.6) cannot be separated experimentally. But the frequency shift due to the second-order Doppler effect can be readily calculated with more than sufficient accuracy, using the existing means available to determine the orbital velocity of the satellite. It thus becomes possible to determine the gravitational frequency shift.

The measured frequency difference (2.6) can be expressed in terms of the elements of the satellite orbit. Assuming the earth's gravitational field to be centrally symmetrical and disregarding the gravitational fields of the other members of the solar system, the satellite orbit is strictly elliptical. If  $a$  is the major semi-axis of the orbit and  $e$  is its eccentricity, then the distance from the center of the earth to the satellite is

$$r = \frac{a(1-e^2)}{1+e \cos \theta}, \quad (2.8)$$

and its velocity is

$$v = \frac{2\pi a}{TV \sqrt{1-e^2}} \sqrt{1+2e \cos \theta + e^2}, \quad (2.9)$$

where

$$T = 2\pi \sqrt{\frac{a^3}{GM_3}} \quad (2.10)$$

is the period of the satellite orbit.<sup>79</sup> In these formulas  $\theta$  is the angle between radii drawn from the earth's center to the orbit perigee and to the satellite,  $G = 6.670 \times 10^{-8} \text{ cm}^3 \text{ g}^{-1} \text{ sec}^{-2}$  is the gravitational constant and  $M = 5.98 \times 10^{27} \text{ g}$  is the mass of the earth. The gravitational frequency shift is

$$\Phi = \frac{\varphi_2 - \varphi_1}{c^2} = \frac{GM_3}{c^2} \left( \frac{1}{r_1} - \frac{1}{r_2} \right), \quad (2.11)$$

where

$$\varphi = -\frac{GM^3}{r} \quad (2.12)$$

is the potential of the gravitational field at a distance  $r$  from the center of the earth; the subscripts 1 and 2 pertain to the point of observation and to the satellite, respectively ( $r_1 = 6.37 \times 10^8 \text{ cm}$  — earth radius). Using these formulas, we can write for the relative value of the measured frequency difference (2.6)

$$\begin{aligned} \frac{\Delta f}{f} &= 2\Phi - \beta^2 \\ &= 1.4 \cdot 10^{-9} \left[ 1 - \frac{r_1}{a(1-e^2)} (1.5 + 2e \cos \theta + 0.5e^2) \right], \quad (2.13) \end{aligned}$$

$$2\Phi = 1.4 \cdot 10^{-9} \left[ 1 - \frac{r_1(1+e \cos \theta)}{a(1-e^2)} \right], \quad (2.13a)$$

$$-\beta^2 = -1.4 \cdot 10^{-9} \frac{r_1(0.5 + 0.5e^2 + e \cos \theta)}{a(1-e^2)}. \quad (2.13b)$$

Thus, the measured frequency difference  $\Delta f$  is periodic in the angle  $\theta$ , and consequently in the time. The maximum of  $\Delta f/f$  is at the apogee and the minimum at the perigee. The difference between these values of  $\Delta f/f$  (double the amplitude of the relative frequency change) is

$$\left( \frac{\Delta f}{f} \right)_{ap.} - \left( \frac{\Delta f}{f} \right)_{per} = 5.6 \cdot 10^{-9} \frac{er_1}{a(1-e^2)}. \quad (2.14)$$

From (2.13a) and (2.13b) we see that the changes in  $2\Phi$  and  $-\beta^2$  with change in  $\theta$  are equal in amplitude and in phase. They therefore make an equal contribution to the overall relative frequency change (2.14).

For a circular orbit ( $e = 0$ ) expression (2.13) goes over into

$$\frac{\Delta f}{f} = 1.4 \cdot 10^{-9} \left( 1 - \frac{1.5}{1 + \frac{h}{r_1}} \right), \quad (2.15)$$

where  $h = a - r_1$  is the height of the satellite above the earth. This is twice the value obtained in reference 4 for a circular orbit, the difference resulting from the use of two-way radio communication with the satellite to eliminate the first-order Doppler effect.

The value of (2.14) increases with increasing eccentricity; to measure the gravitational frequency shift it is therefore convenient to have a highly elongated elliptic satellite orbit.

Assume that the satellite moves on an orbit with a minimum height above the earth  $h_{\min} = 300 \text{ km}$  and a maximum height  $h_{\max} = 10,000 \text{ km}$ . For such an orbit,  $a = 11,520 \text{ km}$  and  $e = 0.423$ . According to (2.13), the relative frequency shift  $\Delta f/f$  varies from  $-9 \times 10^{-10}$  at the perigee to  $+7 \times 10^{-10}$  at the apogee. The total change in the frequency shift is, according to (2.14),  $1.6 \times 10^{-9}$ . The greatest satellite orbital velocity, given by (2.9), is  $9.24 \text{ km/sec}$ . The corresponding relative frequency shift due to the first-order Doppler effect is approximately  $3 \times 10^{-5}$ , some four orders of magnitude greater than the frequency shift due to the summary action of the second-order Doppler effect and the gravitational effect. According to (2.10), the period of the satellite is 3 hours and 25 minutes.

In the two-way radio communication method it is assumed that the signal is transmitted and received at practically the same frequency. This is impossible, in the case of continuous radiation of signals from the earth and from the satellite, if one antenna or two closely-spaced antennas are used for the reception and transmission of the signals in each of these points. Owing to the large distance between the earth and satellite, the transmitted and received signal powers will differ by approximately ten orders of magnitude. For normal operation of the radio receiver it is necessary

that the received signal be much stronger than the signal from the local transmitter. Therefore the electric decoupling between the output of the transmitter and the input of the receiver at each point must be not less than 120 db. This can be realized only by using separate antennas for transmission and reception, and by spacing the antennas far enough apart.

A pulse method<sup>80</sup> has been proposed for two-way radio communication at identical frequencies by staggering the reception and transmission. Single pulses of 1 to 10 μsec duration are received on the satellite, stored in a delay line for a time equal to the duration of the pulse and the time necessary to switch the apparatus from a reception to transmission, and then radiated to the earth. A block diagram of the satellite apparatus is shown in Fig. 18. The signal frequency is chosen in the range from 500 to 1000 Mc/s, primarily owing to the need of using semiconductor devices in the apparatus. For distances up to 16,000 km, the average satellite transmitter power should be about 20 milliwatts, with an approximate peak of 0.4 watt.

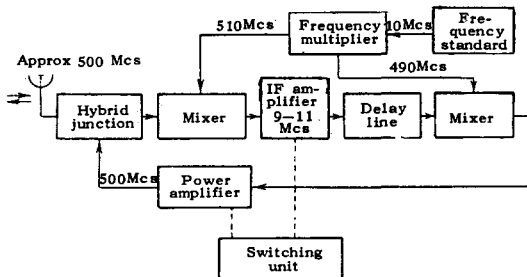


FIG. 18. Block diagram of apparatus mounted on the satellite.<sup>5</sup>

It is proposed to mount on a satellite three sets with generators operating at different frequencies and having different temperature coefficients of frequency, so as to eliminate the systematic errors due to the changes in the temperature as the satellite moves in and out of the earth's shadow. The total power consumed on the satellite will be of the order of 3 watts, and the entire apparatus with batteries will weigh about 16 kg.<sup>80</sup>

A block diagram of the apparatus on earth is shown in Fig. 19. The receiver incorporates a delay discriminator to eliminate the influence of the transmitter signals on the reception. The frequency standards on

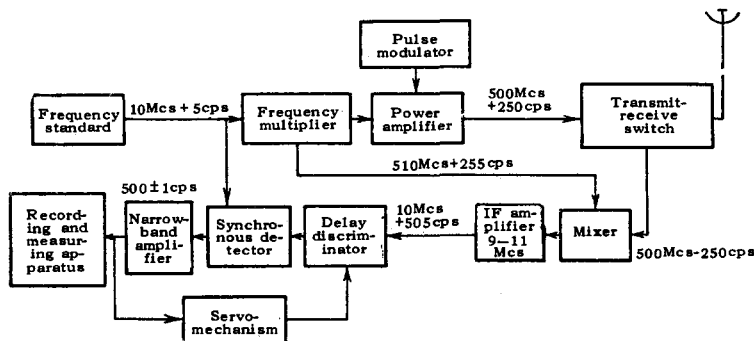


FIG. 19. Block diagram of the apparatus on earth.<sup>5</sup>

earth and on the satellite are shifted in frequency by an amount on the order of 10<sup>-6</sup>. This allows the received signal to be separated from the noise with a narrow-band filter, without affecting appreciably the result of the elimination of the first-order Doppler effect, as can be seen from (2.7). The narrow reception bandwidth permits the use of a low-power transmitter on the satellite. To the contrary, the signal received on the satellite, from which the Doppler effect is not eliminated, is amplified in a broad band of frequencies and a large signal to noise ratio is obtained by using high transmitter power on earth. For an earth antenna with an area of 10 m<sup>2</sup> the transmitter power should be about 500 watts average and 10 kilowatts in pulse.<sup>80</sup>

To eliminate the first-order Doppler effect it is very important that the random fluctuations of the electric length of the signal paths from the earth to the satellite and back be small or well correlated with each other. It is known that radio-wave phase fluctuations are produced in the turbulent inhomogeneities of the troposphere and in the F<sub>2</sub> layer of the ionosphere.<sup>81-85</sup>

Tropospheric fluctuations are produced by changes in the dielectric constant ε of the air. This change, Δε<sub>0</sub>, is very small compared with the mean value of ε<sub>0</sub> along the path of the radio waves, a value very close to unity (Δε<sub>0</sub>/ε<sub>0</sub> ≪ 1 and ε<sub>0</sub> ≈ 1). According to reference 81, it is assumed that the inhomogeneities of the dielectric constant (ε = ε<sub>0</sub> + Δε<sub>0</sub>) and hence of the refractive index (n = √ε ≈ √ε<sub>0</sub> + Δε<sub>0</sub>/2) are isotropically distributed in the troposphere in the form of individual "lumps" and "pockets," with average characteristic dimension l<sub>0</sub>. The length of the electric path in the medium experiences many random changes, so that the total phase fluctuations equal to the sum of the individual phase changes over the entire path of radio wave propagation. The phase fluctuation ψ<sub>0</sub> can be written in the form

$$\psi_0 = \frac{2\pi}{\lambda} \int_0^L (n - n_0) dl = \frac{\pi}{\lambda} \int_0^L \Delta\epsilon_0(l) dl, \quad (2.16)$$

where λ — length of the radio waves, n = √ε<sub>0</sub>, and L — effective thickness of the layer of turbulent inhomogeneities in the troposphere. The average value of ψ<sub>0</sub> is zero. The dispersion of ψ<sub>0</sub> is

$$\overline{\psi_0^2} = \frac{\pi^2}{\lambda^2} \int_0^L \int_0^L \overline{\Delta \epsilon_0^*(l_1) \Delta \epsilon_0(l_2)} dl_1 dl_2. \quad (2.17)$$

The statistical properties of the dielectric constant in the troposphere are determined from the expression

$$\overline{\Delta \epsilon_0^*(l_1) \Delta \epsilon_0(l_2)} = |\Delta \epsilon_0|^2 C(|l_{12}|), \quad (2.18)$$

where the spatial correlation function  $C(|l_{12}|)$  depends only on the distance  $|l_{12}|$  between the two points at which the simultaneous changes in dielectric constant are respectively  $\Delta \epsilon_0(l_1)$  and  $\Delta \epsilon_0(l_2)$ . The experimental data<sup>81</sup> point to an exponential spatial correlation function

$$C(|l_{12}|) = \exp \left[ -\frac{|l_{12}|}{l_0} \right]. \quad (2.19)$$

In the direction of wave propagation we have  $l_{12} = l_1 - l_2$ . From (2.17), (2.18), and (2.19) we calculate the total mean square phase fluctuation  $\psi$ :

$$\psi = \sqrt{\overline{\psi_0^2}} \approx \frac{\sqrt{2l_0 L \pi \Delta \epsilon}}{\lambda} \text{ when } L \gg l_0, \quad (2.20)$$

where  $\Delta \epsilon = \sqrt{(\Delta \epsilon_0)^2}$  — mean squared variation of the dielectric constant of the air in the troposphere.

For a cloudless atmosphere, the numerical values in (2.20) are

$$l_0 \approx 60 \text{ m}, \quad L = 6000 \text{ m}, \quad \Delta \epsilon \approx 10^{-6}.$$

The phase fluctuation (2.20) amounts to

$$\psi \approx 9 \cdot 10^{-12} f \text{ rad},$$

where  $f$  is the signal frequency in cps. In the presence of rain clouds the phase fluctuations increase. In this case  $l_0 \approx 6 \text{ m}$ ,  $L \approx 1500 \text{ m}$ , and  $\Delta \epsilon \approx 20 \times 10^{-6}$ . Then

$$\psi \approx 2.8 \cdot 10^{-11} f \text{ rad}.$$

The phase fluctuations obtained experimentally in reference 82 for 30-cm radio waves propagating in the troposphere agree with the foregoing figures. The large fluctuations reached a value  $\psi \approx 10^{-10} f$  radians, but lasted on the average about one hour, whereas the phase fluctuations over a time on the order of one minute amounted to approximately  $5 \times 10^{-12}$  radian.

Ionospheric phase fluctuations are brought about by changes in the electron concentration. The turbulent inhomogeneities in the  $F_2$  layer are strongest at midnight, local time. According to reference 84, it is assumed that the turbulent inhomogeneities of the electron concentration are isotropically distributed in the ionosphere and have a mean characteristic dimension  $h_0$ . The influence of the magnetic field on the form and on the distribution of the inhomogeneities is disregarded. Then the phase fluctuation  $\psi_0$  can be calculated as for the troposphere:

$$\psi_0 = \frac{2\pi}{\lambda} \int_0^H (n - n_0) dh = \lambda r_e \int_0^H \Delta N(h) dh, \quad (2.21)$$

where the refractive index  $n$  for the radio waves and its mean value  $n_0$  along the propagation path in the ionosphere are very close to unity:

$$n = n_0 - \Delta n, \quad n_0 = 1 - \frac{\lambda^2 r_e N}{2\pi}, \quad \Delta n \approx \frac{\lambda^2 r_e \Delta N(h)}{2\pi} \ll 1,$$

$r_e = 2.8 \times 10^{-15} \text{ m}$  is the classical radius of the electron,  $N$  is the mean electron concentration in the ionosphere,  $\Delta N(h)$  is the deviation of the electron concentration in the turbulent inhomogeneities from its mean value  $N$ , and  $H$  is the thickness of the ionosphere layer. As before,  $\psi_0 = 0$  and the dispersion of  $\psi_0$  is

$$\overline{\psi_0^2} = \lambda^2 r_e^2 \int_0^H \int_0^H \overline{\Delta N(h_1) \Delta N(h_2)} dh_1 dh_2. \quad (2.22)$$

The correlation function of the deviations  $\Delta N$  of the electron concentration from the mean value has the form

$$\overline{\Delta N(h_1) \Delta N(h_2)} = |\overline{\Delta N}|^2 \exp \left[ -\frac{|h_1 - h_2|}{h_0} \right]. \quad (2.23)$$

Therefore the total mean squared ionospheric phase fluctuation  $\psi$  is

$$\psi = \sqrt{\overline{\psi_0^2}} \approx \lambda r_e \Delta N \sqrt{2h_0 H} \text{ when } H \gg h_0. \quad (2.24)$$

The approximate numerical values in (2.24) are  $h_0 \approx 1 \text{ km}$ ,  $H \approx 5 \text{ km}$ , and  $\Delta N \approx 10^{11} \text{ m}^{-3}$  for large fluctuations during strong solar activity. This yields

$$\psi \approx 8.8 \cdot 10^8 f^{-1} \text{ rad},$$

where  $f$  is the signal frequency in cps. Under normal ionospheric activity, the phase fluctuation is much less than indicated, during the entire daytime from sunrise to sunset. We note that (2.20) and (2.24) have been derived for vertical radiowave propagation. For other directions,  $\psi$  increases as the square root of the secant of the zenith angle. For angles close to  $90^\circ$ ,  $\psi$  increases more slowly and remains finite.

The measurement of the gravitational frequency shift consists of recording the low audio frequency  $\Delta f$ , given by (2.6) and (2.13), and measuring the total phase change  $2\pi t \Delta f$  over a time  $t$  on the order of 10 seconds. Since  $\Delta f/f \approx 10^{-9}$ , we have  $2\pi t \Delta f \approx 6.28 \times 10^{-8} f$  radians. Atmospheric fluctuations permit this value to be measured with accuracy  $\pm \psi$ . For the troposphere, the ratio is

$$\frac{\psi}{2\pi t \Delta f} \approx \frac{2.8 \cdot 10^{11}}{6.28 \cdot 10^8} \approx 4.5 \cdot 10^{-4},$$

that is to say, the accuracy of the measurement of the gravitational frequency shift will be better than  $\pm 0.1$  percent. Actually, in view of the correlation of the fluctuations of the electric path from the earth to the satellite and back, the measurement accuracy will be even higher. Indeed, at maximum distance from the satellite to the earth, say 15,000 km, the approximate round-trip signal time including the delay in the satel-

lite apparatus is  $\tau = 0.1$  sec. During this time the phase fluctuation is less than  $10^{-12}$  f. The horizontal displacement of the satellite relative to the observer is less than 1 km during that time. The corresponding spatial shift of the direction of propagation of the signal in the troposphere at an altitude of 1.5 km does not exceed 0.1 m, which is two orders of magnitude less than the dimension of the tropospheric turbulent inhomogeneity within which the phase shifts are well correlated. Thus, the tropospheric phase fluctuations can be considered to be negligibly small.

For the ionosphere, the ratio is

$$\frac{\psi}{2\pi t \Delta f} \approx \frac{8.8 \cdot 10^8 f^{-1}}{6.28 \cdot 10^{-8} f} \approx 1.4 \cdot 10^{16} f^{-2}.$$

When  $f = 1000$  Mcs we obtain  $\psi/2\pi t \Delta f \approx 0.014$ . However, as a result of the correlation of the electric (round trip) path length fluctuations, the accuracy of the measurements will be higher. The correlated phase fluctuations will be excluded from the value of  $\Delta f$ , just as the first-order Doppler effect is, for both phenomena are equivalent to a change in the effective path length between the observer on earth and the satellite. It has been established by observation (Fig. 14 of reference 84) that during the time of magnetic disturbances the rate of phase variation is approximately  $8\pi$  radians per minute. Assuming the correlation function to be exponential, we have

$$\rho(\tau) = e^{-\omega_0 \tau}, \quad (2.25)$$

where  $\omega_0 = 8\pi/60 = 0.42$  radians per second. The mean square phase fluctuation not eliminated from  $\Delta f$  amounts to

$$\Delta\psi = \psi \sqrt{2(1-\rho)}, \quad (2.26)$$

which yields  $\Delta\psi = 0.285\psi$  when  $\tau = 0.1$  sec. Thus, the total phase change  $2\pi t \Delta f$  can be measured with accuracy  $\pm \Delta\psi$ . For  $f = 1000$  Mcs we obtain

$$\frac{\Delta\psi}{2\pi t \Delta f} \approx 0.004.$$

In this case the measurement accuracy is  $\pm 0.4$  percent. By increasing the measurement time  $t$  to a minute, we can improve the measurement accuracy at 1000 Mcs to  $\pm 0.06$  percent. Obviously, at a higher signal frequency the measurement accuracy increases rapidly, and for the centimeter band the influence of ionospheric phase fluctuations is quite insignificant. In practice the signal frequency can be chosen between  $f = 500$  Mcs and  $f = 1500$  Mcs. The upper limit is determined by the absorption of signal power in the earth's atmosphere.

At low values of  $f$  (in the meter band) the phase fluctuations will be very large. This method of communicating with the satellite can then be used to investigate the turbulent inhomogeneities in the ionosphere.

Two-way radio communication between the point of observation and the satellite using continuous signals

from both transmitters is possible only at different frequencies. Here, too, it is possible to exclude the first-order Doppler effect. The radio communication is similar to that described in reference 5: a signal of stable frequency  $f$  is sent from earth and is received on the satellite at a frequency  $f'$  as given by (2.2). In the satellite-borne apparatus the frequency  $f'$  is multiplied and divided to yield a different frequency,  $kf'$ , where  $k$  is an irreducible fraction with neither numerator nor denominator equal to unity. The oscillations at frequencies  $f'$  and  $kf'$  are coherent, and the phase difference between them, referred to one of these frequencies, is maintained constant. The satellite is equipped with a generator of stable frequency  $F$ , with which the converted signal frequency is mixed, and the new signal with difference frequency

$$f'' = F - kf' \quad (2.27)$$

is transmitted to earth, where it is received at a frequency  $f'''$ , given by (2.4). Thus

$$f''' = \left( F - kf' \frac{1 - \beta \cos \alpha}{\sqrt{1 - \beta^2 + 2\Phi}} \right) \frac{\sqrt{1 - \beta^2 + 2\Phi}}{1 + \beta \cos \alpha}. \quad (2.28)$$

An expansion of this expression in powers of  $\beta$  and  $\Phi$  yields, after discarding all terms other than those containing  $\beta^2$  and  $\Phi$ ,

$$f''' = F - kf' + (F - 2kf')(\beta^2 \cos^2 \alpha - \beta \cos \alpha) + F \left( \Phi - \frac{\beta^2}{2} \right). \quad (2.29)$$

Obviously, the first-order Doppler effect will then be excluded if

$$F = 2kf'. \quad (2.30)$$

In this case the ratio of the satellite and earth signal frequencies is close to  $k$ , and none is close to a harmonic of the other, so that the simultaneously received and transmitted signals can be readily separated even if a single antenna is used in either point. The measured frequency difference is

$$\Delta f = f''' - kf' = kf' (2\Phi - \beta^2). \quad (2.31)$$

This difference is formed when the frequency of the signal received on earth is mixed with  $k$  times the frequency radiated from the earth.

The procedure for measuring the gravitational frequency shift remains the same as before. The influence of tropospheric phase fluctuations on the measurement accuracy will be just as small as in the case of the radio pulse communication at equal frequencies. The effect of ionospheric fluctuations will also be small, although dispersion will cause the correlation on the round-trip path to be less effective. The ionospheric fluctuations of the phase will be determined essentially by the lower of the two frequencies,  $f$  or  $kf$ . However, the measurement accuracy will be additionally affected by the total change in the number of electrons along the path of propagation of the signal from the earth to the satellite, since the electric lengths of

the signal paths are not the same at the frequencies  $f$  and  $kf$ .

Although this circumstance is not connected with inhomogeneities in the ionosphere, it also disturbs slightly the conditions for the elimination of the first-order Doppler effect.

Indeed, the electric path length is

$$D = \int_0^s ndR, \quad (2.32)$$

where

$$n = 1 - \frac{Nc^2r_e}{2\pi f^2} \quad (2.33)$$

is the refractive index of the radio waves at that place in the ionosphere, where the electron concentration is  $N$ . The integral (2.32) is taken along the geometric signal path  $R$  (between the points  $O$  and  $S$ , Fig. 16). As a matter of fact, the first-order Doppler effect is due to the time variation of  $D$  and not of  $R$ . Therefore the quantity  $\beta \cos \alpha$  in (2.28) should be replaced by

$\frac{1}{c} \frac{dD}{dt} = \beta \cos \alpha - A(f)$  for the frequency  $f$  in the numerator and the frequency  $kf$  in the denominator. We then obtain for the measured frequency difference, in lieu of (2.31),

$$\Delta f = f'' - kf = kf \{2\Phi - \beta^2 - A(f)(1 - k^{-2})[1 - \beta \cos \alpha + k^{-2}A(f)]\}, \quad (2.34)$$

where

$$A(f) = \frac{r_e c}{2\pi f^2} \frac{d}{dt} \left( \int_0^s NdR \right). \quad (2.35)$$

It is known<sup>86</sup> that the number of electrons in a vertical column  $1 \text{ cm}^2$  in area and  $300 \text{ km}$  high, extending from the earth's surface to the maximum electron concentration in the ionosphere, is about  $2 \times 10^{13}$ . If the satellite passes in the perigee above the earth observer at this height ( $h = 300 \text{ km}$ ) (Fig. 17) with a velocity  $v \approx 10 \text{ km/sec}$ , then

$$\int_0^s NdR \approx 2 \cdot 10^{13} \cos^{-1} z \text{ cm}^{-2}.$$

but  $v = \frac{d}{dt} (h \tan z)$ , that is,  $d(\tan z)/dt = 1/30 \text{ sec}^{-1}$ .

Therefore

$$\frac{d}{dt} \left( \int_0^s NdR \right) = 2 \cdot 10^{13} \frac{d}{dt} (\cos^{-1} z) = 7 \cdot 10^{11} \sin z \text{ cm}^{-2} \text{ sec}^{-1}.$$

For  $z = 45^\circ$  we obtain

$$A(f) \approx 7 \cdot 10^8 f^{-2},$$

where  $f$  is the signal frequency in cps.

At the apogee the satellite will be situated outside the ionosphere, about  $10,000 \text{ km}$  above the earth, moving with a velocity of about  $4 \text{ km/sec}$ . The number of electrons in a vertical  $1 \text{ cm}^2$  column passing through the entire thickness of the atmosphere is about  $10^{14}$ . In this case we obtain for  $z = 45^\circ$ ,

$$A(f) \approx 4 \cdot 10^7 f^{-2}.$$

The value of the integral  $\int_0^s NdR$  can change with

time, owing to the physical processes occurring in the ionosphere, particularly during sunrise and sunset and during magnetic storms. It is known<sup>86</sup> that during sunrise the critical frequency can change by a factor 2 or 3 within one hour; consequently, the electron concentration can change by 4–9 times. If the entire integral changes likewise, we have

$$\frac{d}{dt} \left( \int_0^s NdR \right) \approx 10^{11} \text{ cm}^{-2} \text{ sec}^{-1}$$

and  $A(f) \approx 10^8 f^{-2}$ . It can be assumed that during magnetic storms the value of  $A(f)$  can increase one order of magnitude. This pertains in particular to regions of intense aurorae (latitude  $60-70^\circ$ ). Thus, in order of magnitude,  $A(f) \approx (10^8 - 10^9) f^{-2}$ . For  $f = 1000 \text{ Mcs}$  we have  $A \approx 10^{-10} - 10^{-9}$ .

Obviously, formula (2.34) can be rewritten with sufficient accuracy in the form

$$\Delta f = f'' - kf = kf [2\Phi - \beta^2 - A(f)(1 - k^2)]. \quad (2.36)$$

Thus, in this method of radio communication (for example, with  $k = \frac{2}{3}$ ) the ionosphere can cause a frequency change of the same order of magnitude as the gravitational frequency shift. This influence of the ionosphere on the accuracy of the measurements of the gravitational frequency shift, unlike the influence of the tropospheric and ionospheric phase fluctuations  $\psi$ , cannot be reduced by increasing the time  $t$  of a single measurement. However, it is greatly decreased when the frequency  $f$  is increased, and becomes small in the centimeter band. Naturally, the closer the value of  $k$  is to unity, that is, the smaller the difference in the signal frequencies radiated from the earth and from the satellite, the smaller this influence.

In the meter band, the ionospheric frequency shift greatly exceeds the gravitational shift; this method of radio communication can therefore be used to investigate the ionosphere, that is, to study the variations

of the integral  $\int_0^s NdR$  in time and in space (sections

in the plane containing the observer and the path of the satellite). It is possible to study in this fashion large-scale ionospheric inhomogeneities and their evolution (cellular waves<sup>87</sup>). At the same time, small turbulent inhomogeneities can be investigated by studying the phase fluctuations  $\psi$ .

Another possible method of radio communication between an observer and the satellite is practically independent of the effect of the ionosphere; the signals are continuously emitted from the earth and from the satellite at nearly equal frequencies in the centimeter band. A maser generates oscillations at about  $10^{-10}$  watt and about  $1.3 \text{ cm}$ . Direct radio communication at these wavelengths is made difficult by the large ab-

sorption of the signal in the atmosphere in the water-vapor absorption band.<sup>105</sup> But at twice this wavelength the absorption is no longer very large and the radio communication is possible.

Assume that two masers at the observation point generate electric oscillations with close frequencies  $f_1$  and  $f_2$ , say equal to the frequencies of the ammonia spectral lines  $J = K = 2$  and  $J = K = 3$ . The signal radioed from the earth has a frequency  $f = (f_1 + f_2)/4$ , stabilized by both masers. The signal frequency received on the satellite is

$$f' = f \frac{1 - \beta \cos \alpha + A(f)}{\sqrt{1 - \beta^2 + 2\Phi}} \quad (2.37)$$

The satellite also carries two masers with the same frequencies  $f_1$  and  $f_2$ , which are used to form two signals with frequencies

$$F_1 = f_1 - f', \quad F_2 = f_2 - f' \quad (2.38)$$

which are radiated to the earth. The signals received on earth will have frequencies

$$F'_1 = F_1 \frac{\sqrt{1 - \beta^2 + 2\Phi}}{1 + \beta \cos \alpha - A(F_1)}, \quad F'_2 = F_2 \frac{\sqrt{1 - \beta^2 + 2\Phi}}{1 + \beta \cos \alpha - A(F_2)} \quad (2.39)$$

Substituting (2.37) and (2.38) into (2.39) and expanding both equations of (2.39) in powers of  $\Phi$ ,  $A$ , and  $\beta$ , retaining the terms linear in  $\Phi$  and  $A$  and quadratic in  $\beta$ , and discarding all other terms we obtain

$$\left. \begin{aligned} F_1 &= f_1 - f + (2f - f_1)(\beta \cos \alpha - \beta^2 \cos^2 \alpha) + f_1 \left( \Phi - \frac{\beta^2}{2} \right) \\ &\quad + (f_1 - f)A(F_1) - fA(f), \\ F'_2 &= f_2 - f + (2f - f_2)(\beta \cos \alpha - \beta^2 \cos^2 \alpha) + f_2 \left( \Phi - \frac{\beta^2}{2} \right) \\ &\quad + (f_2 - f)A(F_2) - fA(f). \end{aligned} \right\} \quad (2.40)$$

On earth the frequencies  $F'_1$  and  $F'_2$  are mixed with the frequency  $f$  of the radiated signal, and a difference is formed

$$\Delta f = F'_1 + F'_2 - 2f = 2f \left[ 2\Phi - \beta^2 + \frac{\delta^2}{f^2 - \delta^2} A(f) \right], \quad (2.41)$$

which does not contain the frequency shift due to the first-order Doppler effect. Here  $\delta = (f_2 - f_1)/2$ .

If  $f_1 = 23,722.6$  Mcs and  $f_2 = 23,870.1$  Mcs, that is, the  $N^{14}H_3$  line frequencies, then the quantity  $\delta^2/(f^2 - \delta^2)$  in (2.41) is approximately equal to  $4 \times 10^{-5}$ . This is almost five orders of magnitude less than the quantity  $1 - k^{-2}$  (with  $k = 2/3$ ) contained in (2.36), if the frequencies  $f$  are the same in both cases. Therefore the effect of the ionosphere on the accuracy of measurement of the frequencies (2.41) is quite insignificant in this radio communication method.

In a practical realization of this method, oscillations of frequency  $f = (f_1 + f_2)/4$  are generated on earth (block diagram, Fig. 20) by a reflex klystron stabilized with two masers using automatic phase control (see Sec. 4 of the preceding chapter). The second harmonic of the klystron frequency is mixed with the frequency of each maser, and the two result-

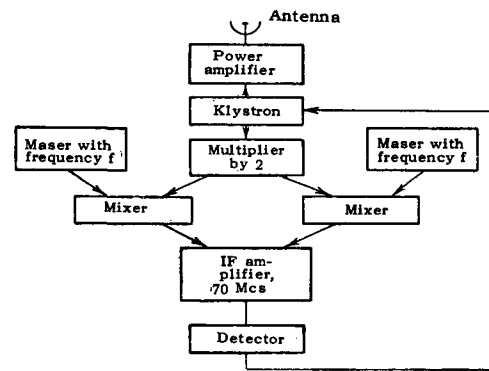


FIG. 20. Automatic phase control of a klystron using two masers.<sup>113</sup>

ant intermediate frequencies  $f_2 - 2f$  and  $2f - f_1$  are amplified in a single amplifier having a bandwidth about 2 Mcs. In the stabilization mode both frequencies are strictly equal to each other and have approximately equal amplitudes. The direct dc output of the detector past the amplifier depends on the phase difference between these two frequencies; the voltage from the detector is fed to the repeller of the klystron, thus closing the stabilization feedback loop. A small change in the klystron frequency immediately causes different changes in the intermediate frequencies, and the resultant change in the phase difference between them changes the voltage on the klystron repeller and returns the klystron frequency to its previous value. The klystron frequency stability will be the same as of the maser, although its generated power is 8 or 9 orders of magnitude greater than that of the maser. At the same time, the frequency of the second harmonic of the klystron differs by several times 10 Mcs from the maser frequencies, and therefore the klystron will hardly affect the values and stabilities of these frequencies.

The radio signal from the klystron is transmitted to the satellite. If the earth antenna directivity coefficient is on the order of  $10^5$ , and that on the satellite is on the order of  $10^3$ , then a 10 watt signal traveling 10,000 km from the earth will have on the satellite about the same power as a maser. This signal, together with one of the masers mounted on the satellite, is used to stabilize the frequency of a klystron,<sup>54</sup> which generates one of the two signals radiated from the satellite to the earth. The block diagram is shown in Fig. 21. The fundamental frequency  $F_1$  of the klystron is mixed with the frequency  $f'$  received from the earth to form an intermediate frequency  $f' - F_1$ . The second harmonic of the klystron frequency  $2F_1$  is mixed with the maser frequency  $f_1$  to form  $f_1 - 2F_1$ . Both intermediate frequencies are amplified by a single amplifier. In the stabilization mode, both frequencies are strictly equal (and therefore  $F_1 = f_1 - f'$ ). The dc output of the detector past the amplifier depends on the phase difference between these frequencies; the detector voltage is fed to the repeller of the klystron.

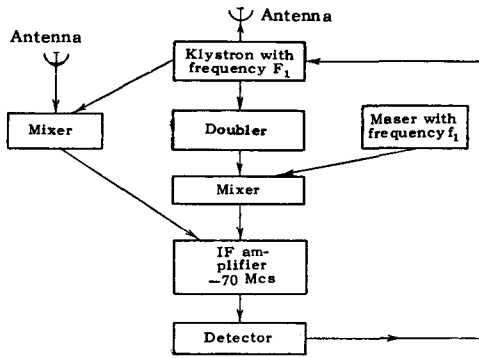


FIG. 21. Automatic phase control of klystron on satellite by means of a maser and a signal from the earth.

A small change in the klystron frequency changes the second intermediate frequency by an amount which is twice the change in the first. This changes the phase difference between them, which changes in turn the voltage on the repeller of the klystron and returns the klystron frequency to the previous value. This brings about automatic phase control of the klystron against the frequency of the signal received on the satellite and against the maser installed on it. The second signal radiated from the satellite is similarly produced with the aid of a second klystron and maser.

The signal received on the satellite differs from each of the radiated signals by approximately 70 Mc/s, the signal frequency being about 12,000 Mc/s. The signals can be transmitted and received with a single antenna, using ferrite decoupling networks and narrow-band filters in the form of stable cavity resonators with a Q on the order of several thousand (for example, cavities made of invar). In addition the receiving channel can carry transmitted and received signals of comparable power, since both are used in the klystron stabilization circuit.

A single antenna can also be used on earth, for the measured frequency difference<sup>41</sup> can be produced by merely mixing the transmitted and received signals. For example, by using a ferrite circulator at the antenna input, it is possible to direct to the detector almost all the received signal power and only a small part of the transmitted signal power. The two intermediate frequencies  $F_2' - f$  and  $f - F_1'$  at the detector output can be amplified in a single amplifier, after which the second detector separates their difference  $\Delta f = F_1' + F_2' - 2f$ , which is determined by the method, described above, of measuring the total phase difference  $2\pi\Delta f$  within a short time  $t$  (on the order of 10 sec).

The power of the signal transmitted from the satellite will be on the order of 0.01 watt and even less. For 0.01 watt and a distance of 10,000 km with a directivity coefficient  $10^3$  for the satellite antenna and  $10^5$  for the earth antenna, the signal power received on earth will be about  $4 \times 10^{-14}$  watt. If the noise factor of the earth receiver is 40, then at a reception band-

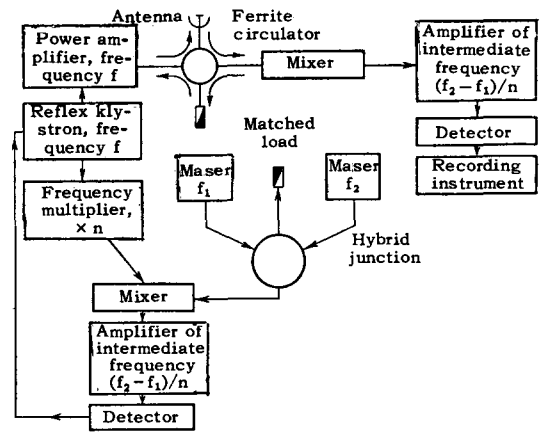


FIG. 22. Block diagram of apparatus on earth with APC of the klystron against the  $n$ -th harmonic.<sup>53</sup>

width of 100 cps the noise power will be approximately  $2 \times 10^{-17}$  watt. The signal to noise ratio is 2000, more than enough to permit the measurements.

In the foregoing method of radio communication between the earth and the satellite, the three frequencies  $f$ ,  $F_1$ , and  $F_2$ , employed are approximately equal to half the maser frequencies. This, naturally, is not an essential condition. The same method can be employed at longer wavelengths. Thus, Fig. 22 shows a block diagram for earth-based apparatus, operating at the frequencies

$$f = \frac{f_1 + f_2}{2n}, \quad F_1 = \frac{2}{n} f_1 - f', \quad F_2 = \frac{2}{n} f_2 - f'. \quad (2.42)$$

Here the  $n$ -th harmonic of the klystron is mixed with the frequency of each maser and the two intermediate frequencies obtained,  $f_2 - nf$  and  $nf - f_1$ , which are exactly equal in the stabilization mode, are amplified in a single amplifier. The ferrite circulator connected at the input of the antenna causes almost all the amplified power at frequency  $f$  to be radiated in space. Only a small part of the power will enter into the mixer of the receiving part of the apparatus, owing to slight reflection from the antenna, depending on its matching with the circulator. This power, however, is sufficient for effective conversion of the frequencies  $F_1'$  and  $F_2'$  of the received signals, practically the total power of which will be directed by the same circulator into the mixer of the receiving part of the apparatus. The converted signal frequencies  $F_2' - f$  and  $f - F_1'$  are amplified in a single amplifier, after which a detector separates their difference, which does not contain any shift due to the first-order Doppler effect. This frequency difference is measured by the method described above, that of registering the total phase difference within the time  $t$  required for a single measurement.

A block diagram of the corresponding apparatus on the satellite is shown in Fig. 23. Here the  $n$ -th harmonic of the klystron frequency  $F_1$  is mixed with the maser frequency. The resultant intermediate fre-

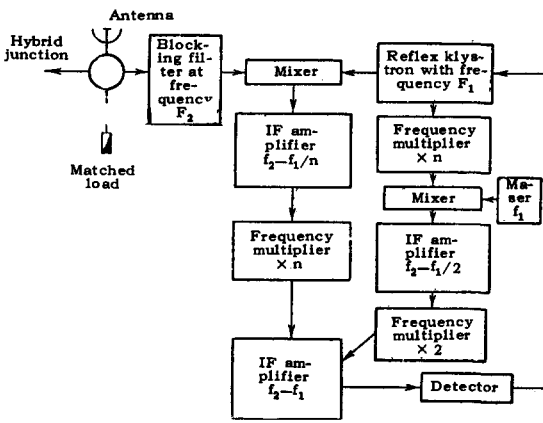


FIG. 23. Block diagram of apparatus on satellite with APC of the klystron against the  $n$ -th harmonic, with odd  $n$  (see reference 53).

quency is amplified and doubled to  $2(f_1 - nF_1)$  after which it is fed to the common amplifier. On the other side, the frequency  $F_1$  is mixed with the signal frequency  $f'$  received on the satellite and the  $n$ -th harmonic of the resultant intermediate frequency  $n(f' - F_1)$ , is also fed to the common amplifier. In the stabilization mode both intermediate frequencies are kept strictly equal to each other in the common amplifier, and the phase difference between them determines the voltage fed to the closed feedback circuit to the klystron repeller to stabilize the klystron frequency. Part of the klystron power to the mixer is also fed to the antenna and is radiated to earth. At the same time, all of the power fed to the mixer is used there, owing to the difference in frequency between the klystron and the received signal. It was shown earlier that the power radiated from the satellite can be sufficiently small, in view of the possibility of using narrow-band filters in the earth receiver. The matched load in the hybrid junction of Fig. 23, just as in Figs. 22 and 24, can be replaced by a second antenna or by a component of the same antenna (say a second dipole in a parabolic mirror) to produce the necessary antenna directivity and polarization.

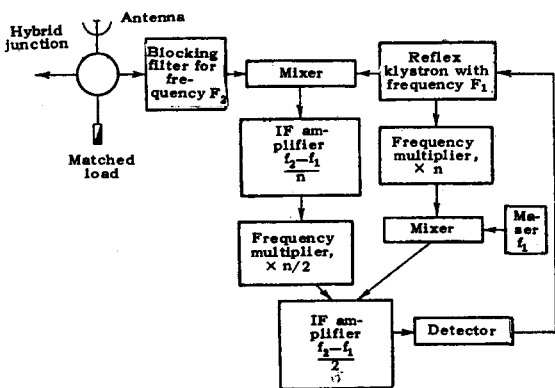


FIG. 24. Block diagram of apparatus on satellite with APC of the klystron against the  $n$ -th harmonic, with  $n$  even (see reference 56).

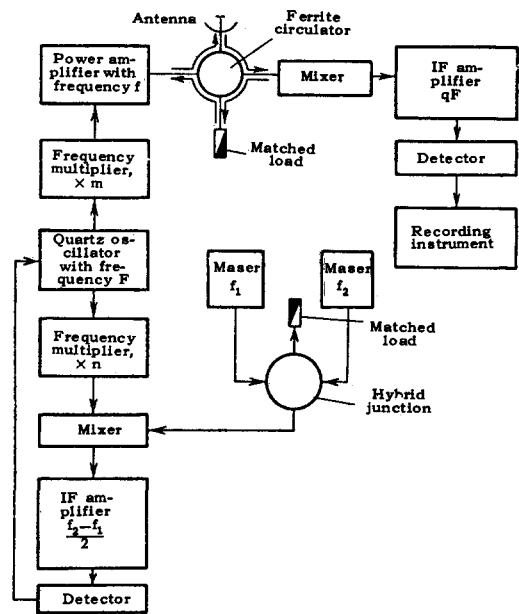


FIG. 25. Block diagram of apparatus on earth, with automatic phase control of the quartz generator by means of two masers.<sup>113</sup>

Figure 23 shows only half of the satellite apparatus. A second similar part generates the frequency  $F_2$  radiated to the earth through the same antenna. The frequency  $F_2$  is prevented from entering the stabilization circuit for the frequency  $F_1$  by a blocking filter tuned to  $F_2$ , in accordance with Fig. 23. An analogous device should be provided to protect the circuit that stabilizes  $F_2$ .

The block diagram shown in Fig. 23 should be used when  $n$  is odd. If  $n$  is even, the block diagram can be simplified as in Fig. 24. In either case the apparatus on earth remains the same, as shown in Fig. 22.

It must be noted that for normal operation of the systems used to stabilize the klystron in the satellite apparatus of either Fig. 21, 23, or 24, the two intermediate-frequency signals obtained by mixing the klystron frequency with the maser frequency on the one hand, and the klystron frequency with the signal received on earth on the other, should have approximately the same amplitudes in their common amplifier. For this purpose automatic control should be provided for the IF amplitude, since this amplitude depends on the distance between the observation point on earth and the satellite. In the absence of a signal from earth, the satellite klystron frequency will not be stabilized and may differ appreciably from its stabilized value. Provision must therefore be made in the satellite apparatus to be able to sweep the unstabilized frequency of the klystrons in a certain range, so that once a signal is received the klystron frequency enters into the locking and holding bands of the stabilization system (APC), after which the sweep circuit is turned off and the klystron frequency left stabilized.



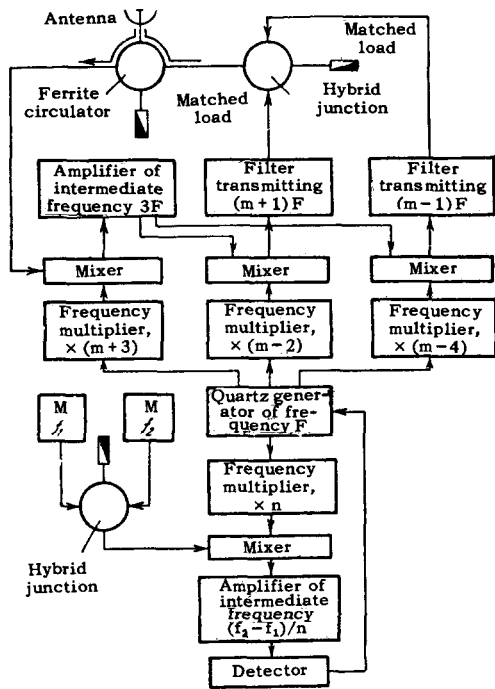


FIG. 26. Block diagram of apparatus on the satellite with APC of the quartz heterodyne by means of two masers.<sup>113</sup>

The klystrons can be successfully replaced with quartz oscillators with much lower frequencies, stabilized by higher maser harmonics. The required small change in the quartz-generator frequency can be made by known methods, say with a reactance tube. In this case the radio communication with the satellite can occur at any harmonic of the quartz heterodyne frequency, say in the short-wave portion of the decimeter band. Figure 25 shows the block diagram of the apparatus on earth, with a quartz generator stabilized by two masers, operating at the following frequencies;

$$f = mF, \quad F_1 = (2m - q)F - f', \quad F_2 = (2m + q)F - f'. \quad (2.43)$$

Here  $F = (f_1 + f_2)/2n$  is the fundamental frequency of the quartz oscillator. In view of the much higher frequency stability of the quartz oscillator compared with a klystron not stabilized with masers, the bandwidth in the feedback circuit used to stabilize the quartz generator can be much narrower than the bandwidth used in the klystron stabilization circuit. This will greatly reduce the noise power in this circuit, and the operation of the frequency stabilization circuit will be steadier. At the same time it is possible to simplify the satellite-borne apparatus. In formulas (2.43)  $q$  need not necessarily be an integer, the specific apparatus used on the satellite may vary, depending on the value of  $q$ . A possible block diagram of this apparatus with  $q = 1$  is shown in Fig. 26. Like the apparatus on earth, it contains only one maser stabilization system. It also differs from the circuits of Figs. 21, 23, and 24 in that

the received signal does not participate in the quartz stabilization and consequently the operating conditions of the stabilization system are independent of the radio communication with the earth. The frequencies  $F_1$  and  $F_2$  are formed only by mixing the quartz harmonics with the signal from the earth. The three multipliers, which increase the frequency by factors  $m+3$ ,  $m-2$ , and  $m-4$  (Fig. 26), can be replaced by a single circuit, which forms narrow pulses of frequency  $F$  and thereby produce a natural series of harmonics, which are multiples of the quartz frequency, with practically equal amplitudes, from which the necessary harmonics are separated by three narrow-band amplifiers. We note also that when ferrite circulators are undesirable or unusable, they can be replaced by combinations of suitable narrow-band filters, or separate antennas can be used for reception and transmission.

In the apparatus of Figs. 25 and 26, the signal power received from the earth and from the satellite need be considerably less than in the apparatus of Figs. 20-24, since the signal received on the satellite is not used to stabilize the quartz frequency. Its power can therefore be much less than that of the maser, and even less than the noise power in the receiver. At a low signal-to-noise power ratio in the satellite apparatus, the mixing, amplification, and filtering of the signal will proceed in normal fashion, in spite of the presence of more noise power than signal power. In the apparatus on earth it is essential to use a large signal-to-noise power ratio ( $\gg 1$ ). This can be ensured by a very narrow reception bandwidth, which can be used here because of the compensation of the first-order Doppler effect and because of the very high frequency stability of the master oscillators. For example, if radio communication is at 10 cm over a distance of 10,000 km, the antenna directivity coefficient is  $10^5$  on earth and  $10^3$  on the satellite, the receiver noise figures on earth and on the satellite are about 10, the bandwidth is 1 Mcps on the satellite and 10 cps on earth, and the total signal power gain on the satellite is  $10^{10}$  (from the antenna input to the antenna output); it is possible to transmit from the earth a  $10^{-5}$ -watt signal and have a signal-to-noise ratio of 0.16 on the satellite and 600 on earth. The signal power from the satellite is then  $6.3 \times 10^{-6}$  watt and the noise power is  $4 \times 10^{-4}$  watt. The use of a very narrow bandwidth (10 cps) in the earth-based receiving apparatus is made possible by converting the intermediate frequency  $qF$  (Fig. 25) into a very low frequency, for which a narrow band filter can be used. The heterodyne necessary for this purpose, with a frequency close to  $qF$ , should have high frequency stability (on the order of  $10^{-8}$ ), obtainable with aid of masers on earth.

For normal operation of the apparatus it is essential that the received signal frequency not be close to any of the heterodyne frequencies or their harmonics, which might enter into the receiver. Total elimination of such interference from the apparatus is possible if

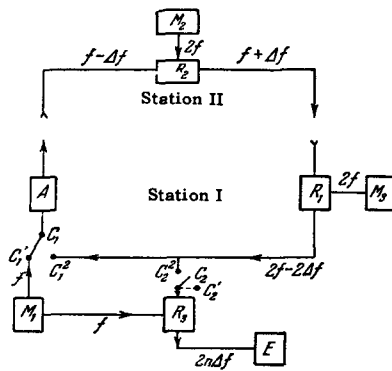


FIG. 27. Experiment to measure the gravitational frequency shift on earth with masers.

the frequencies of the maser-stabilized quartz oscillators are different on earth and on the satellite. For example, if the ratio of the frequency  $F$  of the earth-based quartz oscillator to the frequency  $F_0$  of the quartz oscillator on the satellite is 3:2, then a signal of frequency  $(2p + 1)F$ , where  $p$  is a positive integer, radiated from earth can be mixed in the satellite apparatus with the frequency  $(3p + p)F_0$ , amplified at a frequency  $3F_0/2$ , mixed with the frequencies  $(3p + 1)F_0$  and  $(3p - 1)F_0$ , and filtered down to  $(3p + \frac{1}{2})F_0$  and  $(3p + \frac{5}{2})F_0$ , at which frequencies they are broadcast from the satellite. In this case  $q = \frac{2}{3}$  (see Fig. 25) and communication is at the frequencies given by (2.43), in which we put  $m = 2p + 1$ .

Thus, measurement of the gravitational frequency shift of a maser on a satellite is feasible. Preparations for such an experiment have already been reported.<sup>88</sup>

The gravitational frequency shift near the earth's surface amounts to  $\Delta f/f \approx 10^{-13}$  per kilometer of altitude. The frequency stability of the maser per second of time is of the same order of magnitude. In the very short time intervals needed for the radio waves to travel 1 km from the earth's surface and back, the maser frequency stability can be made much higher. This suggests measurement of the gravitational frequency shift on earth without a satellite, thus eliminating the problems connected with the first and second order Doppler effect.

The idea of the experiment is developed in reference 89; it is based on the radio communication method proposed in reference 5.

Station I (Fig. 27) is located on the earth's surface, while station II is at an elevation  $H$  above it. The maser  $M_1$  in station I oscillates at frequency  $f_1$ , which is amplified in amplifier  $A$  and broadcast to station II, where it arrives at a frequency  $f - \Delta f$ , where  $\Delta f$  is the gravitational shift. From (2.11),

$$\frac{\Delta f}{f} = \frac{GMH}{r^2 c^2}.$$

Receiver  $R_2$  at station II mixes the signal  $f - \Delta f$  with a signal of frequency  $2f$  from maser  $M_2$  and rebroad-

casts the frequency  $2f - (f - \Delta f) = f + \Delta f$ , after filtering and amplification, to station I, where it arrives at a frequency  $f + 2\Delta f$ . In receiver  $R_1$  this frequency is mixed with frequency  $2f$  of maser  $M_3$ , and after filtering and amplification the frequency  $2f - (f + 2\Delta f) = f - 2\Delta f$  is again broadcast to station I. This is done by switching the contactor  $C_1$  from position  $C_1^1$  to signal-transmission position  $C_1^2$  after a time interval  $\tau = 2H/c$  from the start of the operation of maser  $M_1$ .<sup>\*</sup> This switching operation disconnects maser  $M_1$ , which no longer participates in the transmission of the signal. The signal of frequency  $f - 2\Delta f$ , broadcast from station I, arrives at station II at frequency  $f - 3\Delta f$ , where it is mixed, filtered, amplified, and re-broadcast at frequency  $f + 3\Delta f$  to station I, where it is received at frequency  $f + 4\Delta f$ , which is again converted into  $f - 4\Delta f$ , etc.

If  $n$  is the number of complete signal round trips between the stations, the frequency becomes  $f - 2n\Delta f$ , and after the lapse of a time  $t$  its value is  $f - 2t\Delta f/\tau$ . A very small frequency change  $\Delta f$  is thus multiplied by a large number  $2n$  and becomes easier to measure. For this purpose the contactor  $C_2$  is set in position  $C_2^2$ , after which the signal is mixed in receiver  $R_3$  with the oscillations from maser  $M_4$ ; filtering and amplification results in oscillations at a low frequency  $F = 2n\Delta f = 2t\Delta f/\tau$ . The counter  $E$  determines the total number  $N$  of complete cycles of these oscillations. At the end of the measurement time  $T$ , the counter counts  $N$

$$= \int_0^T F dt = T^2 \Delta f / \tau \text{ cycles so that } \Delta f \text{ can be determined}$$

and compared with the calculated value.

For example, if  $H = 3.2$  km, then  $\Delta f/f = 3.4 \times 10^{-13}$  and  $\tau = 2.3 \times 10^{-5}$  sec. The stability of a maser over a time on the order of  $10^{-5}$  sec is better than  $10^{-13}$ . If  $f = 10^{10}$  cps and  $T = 10$  sec, then  $\Delta f = 3.4 \times 10^{-3}$  cps and  $N = 1.5 \times 10^4$  cycles.

## 2. First Order Experiments to Check Special Relativity

The high relative stability of masers makes feasible first-order relativistic experiments (effects linear in  $\beta = v/c$ ) to check the special theory of relativity. At the present time there are two known possible experiments. In the USA a group of radiophysicists led by Townes<sup>91</sup> performed an experiment based on the use of the Doppler effect, proposed by Møller.<sup>92</sup> Another feasible experiment is to measure the phase difference between two unsynchronized masers, which depends on

<sup>\*</sup>We consider here a case when one station is vertically above the other. If the line joining the two stations makes an angle  $\alpha$  with the horizon, then the value of  $\tau$  given in the text must be divided by  $\sin \alpha$ . In addition, we neglect here the delays in the receivers of the two stations. The maser  $M_1$  can be replaced by a block that divides the frequency of maser  $M_1$  by 2.

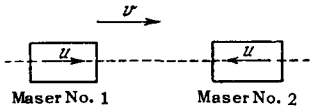


FIG. 28. Relativistic experiment with the Doppler effect.

the rate of propagation of the signal from one maser to the other.<sup>93</sup>

We recall that if we measure the velocity of light in closed circuits, the experiments are of the second and not first order; these include, in particular, all the interference experiments such as Michelson's, and all the experiments which use the synchronization of signals or "clocks" in one form or another.

The experiment in the USA was performed in the following fashion: two masers with horizontal cavities were mounted on a rotating stand; opposing beams of excited ammonia molecules were passed through these cavities (Fig. 28). The frequencies of these masers were compared with each other accurate to  $10^{-12}$ .

Møller<sup>92</sup> analyzed this experiment and calculated the expected frequency change due to  $180^\circ$  rotation of the stand if an absolute reference frame (stationary ether) exists. According to Einstein, the result of the experiment should naturally be negative, that is, when the stand with the masers is turned  $180^\circ$  the relative change in their frequencies should be zero. In such a system, the frequencies, with account of the Doppler shift, are:<sup>92,94</sup>

$$\nu = \nu_0 \left[ 1 + \frac{e u}{c} + \frac{(e u)^2}{c^2} + \frac{v u}{c^2} \right], \quad (2.44)$$

where  $\nu_0$  is the frequency for  $v = 0$ ,  $e$  is a unit vector in the direction of photon emission,  $u$  is the velocity of the molecules, and  $v$  is the velocity of the laboratory in the absolute frame.

This frequency  $\nu$  depends on angle between  $u$  and  $v$ , and the Doppler frequency change is  $\Delta\nu/\nu = uv/c^2$ , neglecting higher-order terms.

This result can be obtained in the following fashion: the laboratory-system formula for the Doppler effect is  $\Delta\nu/\nu = u \cos \theta/c$ , where  $\theta = \pi/2 - v/c$  (aberration angle); if  $v = 0$ , then photons are emitted by the molecules in the cavity in a direction perpendicular to  $u$  ( $u \ll c$ ); if the cavity with the laboratory move with a velocity  $v$  relative to the "ether," then the radiation is directed forward at an angle  $\theta$ , with  $\cos \theta = \sin (v/c) \cong v/c$ , and thus

$$\frac{\Delta\nu}{\nu} = \frac{u}{c} \cos \theta = \frac{uv}{c^2}.$$

Although this term is of second order in  $c$ , it is of first order in  $v/c$ . When the beams are directed oppositely and the apparatus rotated  $180^\circ$ , the magnitude of the effect should be  $4uv/c^2$ .

The orbital velocity of the earth is  $v \sim 30$  km/sec, and the mean thermal velocity of the molecules is  $u \sim 0.6$  km/sec, so that we obtain in this case for the relative change in the maser frequency after rotation through  $180^\circ$ ,

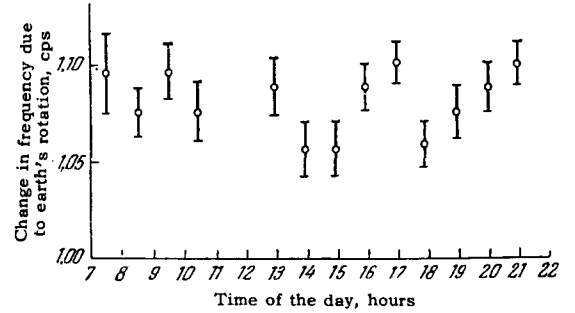


FIG. 29. Variation of the frequency of the two masers in the experiment described in Fig. 28.

$$\frac{\Delta\nu}{\nu} = 4 \frac{uv}{c^2} \cong 4 \frac{6 \cdot 10^4 \cdot 3 \cdot 10^6}{9 \cdot 10^{20}} = 8 \cdot 10^{-10},$$

or

$$\Delta\nu \cong 2.4 \cdot 10^{10} \cdot 8 \cdot 10^{-10} \cong 20 \text{ cps}$$

In this experiment the frequency of the masers differed by several times ten cps and the beat frequency was continuously recorded. After one minute of recording, the apparatus was rotated  $180^\circ$  about its vertical axis from an original orientation along an east-west earth parallel, and the beat frequency in this position again recorded. It must be borne in mind here that to obtain the magnitude of the sought effect it is necessary to take either the sum or the difference of the measurements made at the two positions of the apparatus, depending on the initial detuning  $\Delta\nu/\nu = (\nu_1 - \nu_2)/\nu$  of the two masers. If  $(\nu_1 - \nu_2)/\nu \leq 2uv/c^2$ , the sum of the measurements must be taken; if  $(\nu_1 - \nu_2)/\nu > 2uv/c^2$ , the frequency change is equal to the difference in the measurements in the two positions of the apparatus. This is due to the fact that only the absolute frequency difference is obtained from the comparison of the two maser frequencies. In Townes's experiment<sup>91</sup> about sixteen such measurements with rotation of the entire apparatus were made every hour, while the earth in turn rotated through  $180^\circ$  in twelve hours. The results of the measurements made on September 20, 1958 are shown in Fig. 29 and indicate that, accurate to several hundredths of a cycle, the frequency change is zero, i.e., the observed frequency deviations constitute 1/1000 of the expected effect.

The first series of measurements, carried out on a weekday, when the local magnetic fields and electric interference were intense, showed systematic changes of  $\pm 1/20$  cps daily. The second series of measurements, made on a Saturday, when local interference was negligible, did not disclose changes greater than  $\pm 1/50$  cps. These disturbances were random and were not connected with the orientation of the earth or that of the apparatus.

The measurement accuracy corresponds to a relative maser stability about  $10^{-12}$  over an approximate measurement time of one hour.

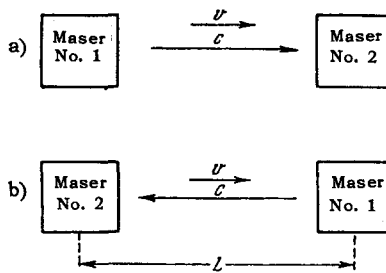


FIG. 30. Arrangement of masers for the measurement of the phase difference. Relativistic experiment of first order.

Another feasible first-order experiment<sup>93</sup> is to measure the phase difference between two unsynchronized masers, placed several meters apart on a rotating mount (Fig. 30). The phase difference between the masers depends on the distance  $L$  between them and on the velocity of propagation of their oscillations. The phase difference between two masers separated by a distance  $L$  is  $\varphi = \omega t = 2\pi L/\lambda$ , where  $\lambda$  is the wavelength, which depends on the phase velocity of the signal ( $\lambda = c_{ph}/\nu$ ) and  $t$  is the time of travel of the signal from the first to the second maser. If the relative signal velocity (the velocity of light) depends on the velocity  $v$  of the receiver ("observer"), then the phase difference should change with a change in the direction of motion. According to Einstein's relativity theory, there should be no changes in the phase difference. A change in the direction of motion can be obtained by rotating the mount with the masers about a vertical axis. Then, if the masers on the mount were initially oriented in the direction of the earth's rotation about the sun and the signal was propagating in the direction of the orbital velocity ( $v$ ) of the earth (Fig. 30a), then after rotation of the mount (Fig. 30b) the signal will propagate in a direction opposite to that velocity. The magnitude of the effect is linear in  $\beta = v/c$  (reference 60). Actually, if the velocity of the signal (light) is not constant, then the time difference between the travel "there" and "back" will be

$$\Delta t = t_1 - t_2 = \frac{L}{c-v} - \frac{L}{c+v} = 2 \frac{L}{c} \frac{\beta}{1-\beta^2} \cong 2 \frac{L}{c} \beta, \quad (2.45)$$

or  $\Delta t/t = 2\beta$ , where  $\beta = v/c$ .

The corresponding change in phase will be

$$\frac{\Delta t}{t} \frac{\Delta \omega}{\omega} = \frac{\Delta \varphi}{\varphi} = 2\beta, \quad (2.46)$$

or  $\Delta \varphi = 2\beta \varphi = 2\beta 2\pi L/\lambda$ . When  $\lambda = 1.25$  cm and  $L = 12.5$  m, we get

$$\Delta \varphi = 2 \cdot 10^{-4} \cdot 2\pi \cdot 10^3 = 0,4\pi,$$

since  $\beta = v/c = 10^{-4}$  for the earth's orbital velocity. Such a phase difference can be readily measured with the circuit of Fig. 31. Here two masers M1 and M2 are coupled through a waveguide (or horn antennas) and beat with a third maser M3, while superheterodyne receivers with a common heterodyne amplify the signals at the intermediate frequency. The phase dif-

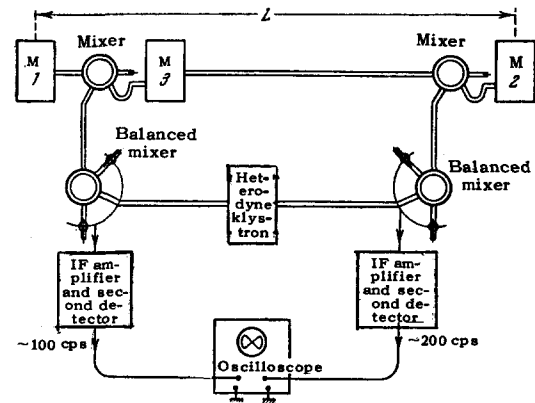


FIG. 31. Diagram of first-order relativistic experiment with two unsynchronized "clocks."

ference between M1 and M2 remains constant in this case and can be determined from the Lissajous figure on an oscilloscope. The frequency difference between M1 and M2 is set at several tens or hundreds of cycles in order to prevent locking. The frequency of the beats between M1 and M2 and between M2 with M3 is set at 1:2 to obtain a figure-eight oscilloscope pattern. If the signal velocity depends on the velocity of the laboratory relative to the "ether," then the form of the Lissajous figure will change as the mount with the masers is rotated in accord with the change in the phase difference  $\Delta \varphi$ .

The relative stability of the two masers used in this experiment must be quite high. Indeed, the phase difference must not change noticeably during the time of the experiment ( $\tau$ ), that is, during the time needed to rotate the mount through  $180^\circ$ , which amounts to several seconds. From this condition we obtain the requirement for the frequency stability

$$\frac{\Delta v}{v} = \frac{\Delta \varphi}{\omega \tau} < \frac{0,4\pi}{2\pi \cdot 2,4 \cdot 10^{10} \cdot 10} \approx 10^{-12},$$

we use here  $\tau = 10$  sec. In a smooth empty waveguide,  $c_{ph} > c$ ; on the other hand if we connect the masers with a loaded or dielectric-filled waveguide, in which  $c_{ph} < c$ , then the accuracy of the experiment can be increased or the distance between masers reduced without reducing the accuracy.

Instead of mounting the masers on a rotating mount with a fixed distance  $L$  between them, we can place one receiver next to each generator and move one of the generators, so as to increase the distance between them. If the velocity of the signal in the "forward" and "backward" directions is not the same, then the phase differences measured at the locations of the first and second generators will not increase by the same amount as the path  $L$  is increased by an amount  $l$ , and the difference in this increase in the phase difference will be given by the same formula as before,

$$\Delta \varphi = 2\beta \varphi = 2\beta \cdot 2\pi \frac{l}{\lambda}.$$

In this case the two masers, equipped with trans-

mitting and receiving antennas, can be moved apart a much greater distance ( $l > L$ ) than when a rotating base is used, and the magnitude of the measured effect and the accuracy of the experiment will be appreciably increased. But maser power will no longer be sufficient, and it will become necessary to employ klystrons with APC maser stabilization (see Chap. I, Sec. 4).

**III. USE OF ATOMIC AND MOLECULAR FREQUENCY STANDARDS FOR THE INVESTIGATION OF COSMOLOGICAL EFFECTS**

Development of high-stability atomic clocks makes feasible an experimental verification of certain cosmological hypotheses, connected with the structure of space, time, and the nature of gravitation.

These questions are dealt with in a paper by Dicke.<sup>3</sup> The results of this paper will be abstracted below, but we must make a few preliminary remarks.

It is known that general relativity singles out certain coordinate systems.<sup>63</sup> In an analysis of the space-time metric of the universe, such coordinate systems are singled out by specifying the boundary conditions on the metric tensor  $g_{ik}$  at infinity. Namely, the boundary values of  $g_{ik}$  should be specified through the material tensor  $T_{ik}$ ; in particular, if there are no masses at infinity (speaking more accurately, if the mass density in the universe decreases sufficiently rapidly with distance) the boundary values  $g_{ik}$  should become equal to the Galilean values.

V. A. Fock, in particular, solved the problem of singling out such a special reference frame by introducing harmonic coordinates.<sup>93</sup>

Specially defined reference frames are characteristic also of classical gravitational theory. In this case the absolute acceleration of the bodies must be replaced by acceleration relative to the masses remaining in the universe (the so-called "Mach principle"). From this point of view, the inertia of a body should be determined by the distribution of the remaining masses in the universe and should vanish when these masses are removed.

Dicke<sup>3</sup> considered, as an example of the development of this point of view, the acceleration of the earth relative to the sun. According to Newton's law, the acceleration is proportional to  $m/r^2$ , where  $m$  is the mass of the sun and  $r$  is the distance from the earth to the sun. It can be assumed that this expression fully describes the dependence of the acceleration on  $m$  and on  $r$  in the first approximation. By introducing the cosmogonic quantities, namely the mass of the universe  $M$ , its radius  $R$ , and the velocity of light  $c$ , we can write for the acceleration  $a$

$$a = \gamma \frac{m Rc^2}{r^2 M}, \tag{3.1}$$

where  $\gamma$  is a dimensionless constant on the order of unity. It is seen from (3.1) that the gravitational constant  $g$  can be determined in terms of the radius, the

mass of the universe, and the velocity of light in the following fashion:

$$g = \gamma \frac{Rc^2}{M}. \tag{3.2}$$

It is thus seen that the gravitational constant depends on the structure of the universe, and can, in particular, vary with time. Formula (3.2) naturally neglects local changes in the gravitational constant  $g$  that can occur near individual masses. It is to be expected that these local changes can be accounted for by further expansion of the expression for  $g$  in powers of  $m/M$  and  $r/R$ , so that

$$\delta g^{-1} = \frac{m}{rc^2}. \tag{3.3}$$

This amounts to  $\sim 10^8$ . It is seen from (3.2) that the gravitational constant  $g$  can vary with time; in particular, in the case of an expanding universe, according to Dirac's estimates, we can expect the gravitational constant to change annually by an amount of the order of

$$\delta g = g \cdot 10^{-10}. \tag{3.4}$$

This change in the gravitational constant can apparently be observed by comparing the movement of a high-accuracy atomic clock with the period of rotation of a satellite, since the latter varies with the gravitational constant as  $\tau = 1/g^2$ .

Another possible cause of change in the gravitational constant is the eccentricity of the earth's orbit. Estimates based on formula (3.3) yield for the annual change in  $g$  a value

$$\frac{\delta g}{g} = 10^{-10}. \tag{3.5}$$

The question also arises of the possible time dependence of other physical quantities, such as the fine-structure constant  $\alpha = e^2/\hbar c$ . In accordance with the ideas developed in references 96 and 97, a point-like interaction in quantum field theory actually leads to absence of any interaction when the energies are not too high, as is the rule in the experiments. This means that the physical charge of the electron is theoretically equal to zero, i.e., we have  $\alpha = 0$  in lieu of the experimental  $\alpha = 1/137$ . One of the possible ways out of this dilemma is to "cut off" the electromagnetic interaction at a certain minimum length  $\lambda$ . In particular, we can assume  $\lambda$  to be the gravitational length

$$\lambda = \left( \frac{g\hbar}{c^3} \right)^{\frac{1}{2}} \approx 10^{-33}. \tag{3.6}$$

In this case the value of the fine-structure constant will depend on  $\lambda$ , and consequently on  $g$ , so that  $\alpha \rightarrow 0$  as  $g \rightarrow 0$ .

From the results of reference 96 we can obtain a numerical estimate of the change in the fine structure constant,

$$\frac{\delta \alpha}{\alpha} \approx 10^{-2} \frac{\delta g}{g}. \tag{3.7}$$

This change in  $\alpha$  can be verified experimentally by comparing the movement of two atomic clocks of different types, since the frequency of each type of clock can depend differently on the fine structure constant  $\alpha$ . Atomic and molecular clocks operating on cesium and on ammonia, respectively, are suitable for this purpose, since the energy levels corresponding to the transition frequencies are produced in these two cases by different interaction mechanisms.

Another series of experiments can be suggested for a clarification of the nature of gravitation, and is a logical continuation of the experiments of Majorana<sup>38</sup> on the screening of gravitational fields. Obviously, in light of the foregoing, if screening of the gravitational field does indeed take place, we can expect the movement of an atomic clock to change when it is screened by a heavy mass.

## CONCLUSION

The described experiments aimed at verification of the general theory of relativity are very difficult to perform, for they require exceedingly complicated apparatus, operating reliably and automatically on satellites or space rockets. An exact measurement of the gravitational frequency shift necessitates also a further increase in the absolute and relative frequency stability of molecular and atomic devices. The feasibility of such experiments in principle, however, has attracted the attention of many researchers and it is hoped that such experiments will be realized in the nearest future.

The placing of molecular or atomic devices on artificial satellites or space rockets will also help solve many important problems in interplanetary navigation, and to ascertain the conditions under which high-stability electromagnetic oscillations propagate through the ionosphere and the terrestrial atmosphere. Valuable data will be obtained, incidentally, on the structure of the ionosphere and of the atmosphere.

The possible experiments described in Chap. III are not yet rigorously motivated, since they are all based on various hypotheses and assumptions, and represent merely the first attempts at exploring the possibility of verifying certain cosmogonic hypotheses by methods of quantum radiophysics. There is no doubt that many more experiments aimed at this purpose will be proposed.

The question of such experiments becomes meaningful because hyperfine atomic and molecular clocks with absolute frequency stability on the order of  $10^{-10}$  and better<sup>39</sup> have become feasible. However, the effects considered in the article are on the present-day borderline of time-measurement accuracy, and an experimental verification of these effects will greatly depend on the progress in the development of super-stable oscillators.

## APPENDIX

### DERIVATION OF FORMULA FOR RELATIVISTIC RED SHIFT OF THE FREQUENCY OF A SPECTRAL LINE

The Einstein effect can be obtained by means of simple calculations for the simplest case of one stationary spherical mass  $M$ . In this case the stationary mass that creates the gravitational field is assumed to be much greater than the mass moving in the gravitational field, so that the reaction of the latter on the gravitational field is negligible.

The space-time interval in the field of a spherical mass has been first determined by Schwarzschild and has the form<sup>37,38</sup>

$$ds^2 = g_{ik} dx^i dx^k = c^2 \frac{r-\alpha}{r+\alpha} dt^2 - \frac{r+\alpha}{r-\alpha} dr^2 - (r+\alpha)^2 [d\theta^2 + \sin^2 \theta d\varphi^2], \quad (1)$$

where  $\alpha = GM/4\pi c^2$ ,  $G$  is Newton's gravitational constant, and  $c$  is the velocity of light in vacuum; the origin is at the center of the body  $M$ . Even this expression for the interval shows that, for a stationary clock ( $dr = r d\theta = r d\varphi$ ), the periodic processes in the presence of the mass are slower than in a space with a Galilean metric, namely:

$$d\tau_1 = \frac{r-\alpha}{r+\alpha} dt = \left(1 - \frac{2\alpha}{r}\right) dt, \quad (2)$$

since usually  $\alpha/r \ll 1$ .

Here  $d\tau_1$  is the interval between two ticks of the clock in the gravitational field, if  $dt$  is the corresponding interval for the same clock outside the gravitational field. The quantity  $c^2\alpha/r$  is none other than the potential of the gravitational field  $\varphi$  at the point  $r$ , so that the difference between the readings of identical clocks placed at different points of the field depends on the difference in the field potentials at these points:

$$\frac{\Delta\tau}{\tau} = \frac{\varphi_1 - \varphi_2}{c^2}. \quad (3)$$

The motion of the body in the gravitational field establishes a definite connection between the differentials of the coordinates, which can be determined by solving the equation of motion of the mass in the gravitational field:

$$\frac{d^2 x^i}{ds^2} = \Gamma_{\alpha\beta}^i \frac{dx^\alpha}{ds} \frac{dx^\beta}{ds}. \quad (4)$$

The solution of (4) for the case when the metric tensor is given by (1) can be found, for example, in the books by Eddington,<sup>39</sup> Fock,<sup>38</sup> and Pauli.<sup>40</sup> From this solution it follows that for a body moving in the gravitational field we have

$$ds = \frac{c}{v} \left( \frac{r-\alpha}{r+\alpha} \right)^{\frac{1}{2}} dt. \quad (5)$$

The parameter  $\epsilon$  is expressed in terms of the eccen-

tricity of the orbit  $e$  and the total angular momentum  $\mu$ :

$$e^2 = 1 - \alpha^2 \frac{c^2}{\mu^2} (1 - e^2). \quad (6)$$

Expression (5) in conjunction with (6) gives us the proper time in a coordinate system at rest relative to the mass  $m$  (of the satellite).

For a circular orbit,  $e^2 = 0$ , we obtain the expression given in reference 41.

The proper time shown by the clock resting on earth (mass  $M$ ) can be calculated from formula (2), where we set  $r$  equal to the earth radius  $R_e$ . Then the relative difference in the readings of the clocks on the satellite and on earth is

$$\frac{c}{v} \left( 1 - \frac{2\alpha}{r} \right) \left( 1 + \frac{2\alpha}{R_e} \right). \quad (7)$$

The maximum value of (7) is  $\sim 7 \times 10^{-10}$ .

The slowing down of the time in the presence of a gravitational field can be graphically treated by using the principle of equivalence and the concept of a photon having an inertial mass  $m_{ph} = h\nu/c^2$ . By virtue of the equivalence principle, the photons should also have a heavy (gravitational) mass, with value  $m_{ph}$ . But in such a case, after passing through a potential difference  $\Delta\varphi = \varphi_1 - \varphi_2$ , the photon will acquire an energy

$$-m_{ph} \Delta\varphi = -\frac{h\nu}{c^2} \Delta\varphi. \quad (8)$$

Since the photon frequency is uniquely related with energy, we get

$$h\nu_1 = h\nu \left( 1 - \frac{\Delta\varphi}{c^2} \right),$$

or

$$v_1 = v \left( 1 - \frac{\varphi_1 - \varphi_2}{c^2} \right), \quad (9)$$

which corresponds to (3).

It must be noted that this treatment is suitable only in the linear approximation of Einstein's theory, for only in this approximation is the concept of the Newtonian principle meaningful. Nonetheless, the quantitative accuracy of this treatment is sufficiently high, owing to the smallness of the gravitational effects of the general theory of relativity.

<sup>1</sup>R. V. Pound, Paper at Second All-Union Conference on Nuclear Reactions and Low and Medium Energies, July 27, 1960, Moscow State University. [Usp. Fiz. Nauk 72, 657 (1960), Soviet Phys.-Uspekhi 3, 875 (1961)].

<sup>2</sup>R. L. Mössbauer, Z. Physik 151, 124 (1958).

<sup>3</sup>R. H. Dicke, Quantum Electronics Symposium, New York, 1960, p. 572.

<sup>4</sup>S. F. Singer, Phys. Rev. 104, 11 (1956).

<sup>5</sup>Badessa, Kent, and Nowell, Phys. Rev. Lett. 3, 79 (1959).

<sup>6</sup>V. L. Ginzburg, Usp. Fiz. Nauk 59, 11 (1956). Collection: Эйнштейн и современная физика (Einstein and Modern Physics), Gostekhizdat, 1956, pp. 93-139.

<sup>7</sup>Gordon, Zeiger, and Townes, Phys. Rev. 99, 1264 (1955); Phys. Rev. 95, 282 (1954).

<sup>8</sup>N. G. Basov, Радиотех. и электрон. (Radio Engineering and Electronics) 1, 51 (1956); Приб. и тех. эксп. (Instrum. and Exptl. Techniques) 1, 71 and 77 (1957).

<sup>9</sup>N. G. Basov and A. M. Prokhorov, JETP 27, 431 (1954).

<sup>10</sup>N. G. Basov and A. N. Oraevskii, Изв. вузов (Радиофизика) (News of the Universities, Radiophysics) 2, 63 (1958).

<sup>11</sup>P. Clausing, Ann. Physik 12, 961 (1952).

<sup>12</sup>B. B. Dayton, Vacuum Technik 1 (1958).

<sup>13</sup>Bennewitz, Paul, and Schlier, Z. Phys. 139, 489 (1954).

<sup>14</sup>F. O. Vonbun, J. App. Phys. 29, 632 (1958).

<sup>15</sup>A. F. Krupnov, op. cit. ref. 10, 2, 658 (1959).

<sup>16</sup>K. Karplus and J. Schwinger, Phys. Rev. 73, 1020 (1948).

<sup>17</sup>H. S. Sneider and P. J. Richards, Phys. Rev. 73, 1178 (1948).

<sup>18</sup>L. A. Vainshstein, Электромагнитные волны (Electromagnetic Waves), Soviet Radio Press, 1957.

<sup>19</sup>K. Shimoda, J. Phys. Soc. Japan 12, 1006 (1957); 13, 938 (1958).

<sup>20</sup>N. G. Basov and A. M. Prokhorov, JETP 30, 560 (1955), Soviet Phys. JETP 3, 426 (1955). Doklady AN SSSR 101, 47 (1955).

<sup>21</sup>Shimoda, Wang, and Townes, Phys. Rev. 102, 1308 (1956).

<sup>22</sup>Yu. L. Klimontovich and R. V. Khokhlov, Soviet Phys. JETP 32, 1150 (1957), Soviet Phys. JETP 5, 937 (1957).

<sup>23</sup>Gunter-Mohr, Townes, and Van-Vleck, Phys. Rev. 94, 1191 (1954).

<sup>24</sup>J. P. Gordon, Phys. Rev. 99, 1253 (1955).

<sup>25</sup>N. G. Basov and A. N. Oraevskii, Радиотех. и электрон. (Radio Engineering and Electronics) 4, 1185 (1959).

<sup>26</sup>Basov, Nikitin, and Oraevskii, ibid. 6, 796 (1961).

<sup>27</sup>K. Shimoda, Trans. Conf. on Quantum Electron-Resonance Phenomena, USA: Sept. 1959.

<sup>28</sup>F. S. Barnes, Proc. IRE 47, 2085 (1959).

<sup>29</sup>N. G. Basov and A. N. Oraevskii, JETP 37, 1068 (1959), Soviet Phys. JETP 10, 761 (1960).

<sup>30</sup>L. Essen and J. W. L. Parry, Nature 177, 744 (1956).

<sup>31</sup>Mockler, Beehler, and Barnes, Quantum Electronics, A Symposium edited by C. H. Townes, Columbia University Press, New York, 1960, p. 127.

<sup>32</sup>N. F. Ramsay, Molecular Beams (Russ. Transl.) IL, 1960.

<sup>33</sup>L. Essen, Nature 178, 34 (1956).

<sup>34</sup>N. F. Ramsay, Phys. Rev. 78, 695 (1956).

- <sup>35</sup> Hollowey, Meinberger, Reder, Winkler, Essen, and Parry, *Proc. IRE* **47**, 1730 (1959).
- <sup>36</sup> J. R. Zacharias, *Phys. Rev.* **94**, 715 (1954).
- <sup>37</sup> Kleppner, Ramsay, and Fieldstadt, *Phys. Rev. Lett.* **1**, 232 (1958).
- <sup>38</sup> R. H. Dicke, *Phys. Rev.* **89**, 472 (1953); J. P. Wittke and R. H. Dicke, *Phys. Rev.* **96**, 530 (1954).
- <sup>39</sup> C. V. Heer, *op. cit.* ref. 27.
- <sup>40</sup> W. Smith, *Molecular Beams (Russ. Transl.)*, IL, 1959.
- <sup>41</sup> H. K. Hughes, *Phys. Rev.* **72**, 614 (1947).
- <sup>42</sup> V. W. Hughes, *Rev. Sci. Instr.* **30**, 689 (1959).
- <sup>43</sup> M. E. Zhabotinskii and V. F. Zolin, *op. cit.* ref. 25, **4**, 1943 (1959).
- <sup>44</sup> A. Kastler, *J. Phys. et Radium* **11**, 255 (1950).
- <sup>45</sup> A. Kastler, *J. Opt. Soc. Amer.* **47**, 460 (1957).
- <sup>46</sup> Bell, Bloom, and Williams, *IRE Trans. MTT-7*, **95** (1959).
- <sup>47</sup> S. M. Bergman, *J. Appl. Phys.* **31**, 275 (1960).
- <sup>48</sup> A. C. Schawlow and C. H. Townes, *Phys. Rev.* **112**, 1940 (1958).
- <sup>49</sup> A. W. Warner, *IRE Trans. Instrum.* **7**, 185, 129 (1958).
- <sup>50</sup> A. H. Morgan and J. A. Barnes, *Proc. IRE* **47**, 1782 (1959).
- <sup>51</sup> M. Peter and M. W. P. Strendberg, *Proc. IRE* **43**, 869 (1955).
- <sup>52</sup> M. Kaplanov and V. Levin, *Автоматическая подстройка частоты (Automatic Frequency Control)* GEI, 1956.
- <sup>53</sup> Vasneeva, Gaigerov, Grigor'yants, Elkin, and Zhabotinskii, *op. cit.* ref. 25, **6**, 231 (1961).
- <sup>54</sup> Vasil'eva, Grigor'yants, and Zhabotinskii, Paper at Second All-Union Conf. Ministry of Higher Education USSR, Saratov, September 1957.
- <sup>55</sup> V. V. Grigor'yants and M. E. Zhabotinskii, *op. cit.* ref. 25, **6**, 321 (1961).
- <sup>56</sup> I. L. Bernshtein and V. L. Sibiryakov, *op. cit.* ref. 25, **3**, 288 and 290 (1958).
- <sup>57</sup> Basov, Murin, Petrov, Prokhorov, and Shtranikh, *op. cit.* ref. 10, **1**, 50 (1958).
- <sup>58</sup> S. M. Bergmann, *J. Appl. Phys.* **31**, 275 (1960).
- <sup>59</sup> F. O. Vonbun, *Rev. Sci. Instr.* **31**, 900 (1960).
- <sup>60</sup> S. I. Vavilov, *Experimental Foundations of Relativity*, Coll. Works, vol. 4, AN SSSR, 1956.
- <sup>61</sup> A. S. Eddington, *The Mathematical Theory of Relativity*, Cambridge Univ. Press, 1930.
- <sup>62</sup> P. G. Bergmann, *Introduction to the Theory of Relativity*, Prentice-Hall, N.Y., 1942.
- <sup>63</sup> W. Pauli, *Relativity Theory (Russ. Transl.)* OGIZ, 1947.
- <sup>64</sup> R. V. Pound and G. A. Rebka, *Phys. Rev. Lett.* **4**, 337 (1960).
- <sup>65</sup> V. L. Ginzburg, *Scient. American* **200**, 149 (1959).
- <sup>66</sup> A. Peres, *Nuovo cimento* **15**, 351 (1960).
- <sup>67</sup> L. J. Schiff, *Phys. Rev. Lett.* **4**, No. 5, 215 (1960).
- <sup>68</sup> *Sci. News Lett.* **75**, 19 (10.I.1960).
- <sup>69</sup> G. M. Clemance, *Revs. Modern Phys.* **19**, 361 (1947).
- <sup>70</sup> H. R. Morgan, *Astrophys. J.* **50**, 127 (1945).
- <sup>71</sup> O. Struve, *Sky and Telescope* **13**, 225 (1954).
- <sup>72</sup> C. H. Townes, *J. Appl. Phys.* **22**, 1365 (1951).
- <sup>73</sup> V. L. Ginzburg, *Doklady AN SSSR* **97**, 617 (1954).
- <sup>74</sup> V. L. Ginzburg, *JETP* **30**, 213 (1956), *Soviet Phys. JETP* **3**, 136 (1956).
- <sup>75</sup> V. L. Ginzburg, *Природа (Nature)*, No. 9, 30 (1956).
- <sup>76</sup> N. G. Basov, *Doctoral dissertation*, *Phys. Inst. Acad. Sci.*, 1956.
- <sup>77</sup> V. L. Ginzburg, *Usp. Fiz. Nauk* **63**, 119 (1957).
- <sup>78</sup> V. L. Ginzburg, *Fortschr. Physik* **5**, 16 (1957).
- <sup>79</sup> S. N. Blazhko, *Курс сферической астрономии (Course of Spherical Astronomy)*, OGIZ, 1948.
- <sup>80</sup> Badessa, Kent, Nowell, and Searle, *Proc. IRE* **48**, 758 (1960).
- <sup>81</sup> R. B. Muchmore and A. D. Wheelon, *Proc. IRE* **43**, 1437 (1955).
- <sup>82</sup> J. W. Herbstreit and M. E. Thompson, *Proc. IRE* **43**, 1391 (1955).
- <sup>83</sup> J. L. Pawsey and R. N. Bracewell, *Radio Astronomy*, 1955.
- <sup>84</sup> H. G. Booker, *Proc. IRE* **46**, 298 (1958).
- <sup>85</sup> C. O. Hines, *Proc. IRE* **47**, 176 (1959).
- <sup>86</sup> S. K. Mitra, *The Upper Atmosphere*, Univ. of Calcutta, 1952.
- <sup>87</sup> D. F. Martyn, *Proc. Roy. Soc. A* **201**, 216 (1950).
- <sup>88</sup> *Sci. News Lett.* **76**, 35 (18.VII.1959).
- <sup>89</sup> M. Surdin, *Compt. rend.* **250**, 299 (1960).
- <sup>90</sup> H. W. de Wijn, *Appl. Sci. Res.* **83**, 261 (1960).
- <sup>91</sup> Cedarholm, Bland, Harnes, and Townes, *Phys. Rev. Lett.* **1**, 342 (1959).
- <sup>92</sup> C. Møller, *Nuovo cimento suppl.* **6**, 381 (1957).
- <sup>93</sup> G. M. Strakhovskii, *Lomonosov Lecture*, Moscow State Univ. 1958.
- <sup>94</sup> C. Møller, *The Theory of Relativity*, London, 1952.
- <sup>95</sup> V. A. Fock, *Теория пространства, времени и тяготения (Theory of Space, Time, and Gravitation)*, Gostekhizdat, 1956.
- <sup>96</sup> Landau, Abrikosov, and Khalatnikov, *Doklady AN SSSR* **95**, 497, 773, and 1177 (1954).
- <sup>97</sup> L. D. Landau and I. Ya. Pomeranchuk, *ibid* **102**, 489 (1955).
- <sup>98</sup> Q. Majorana, *Atti Reale Acad. Lincei* **28**, 2 Sem., 165, 221, 313, 416, 580 (1919); **29**, 1 Sem., 23, 90, 163, 235 (1920); **30**, 1 Sem., 75, 289, 350, 442 (1921); **31**, 1 Sem., 41, 81, 141, 221, 343 (1922).
- <sup>99</sup> Basov, Strakhovskii, and Cheremiskin, *op. cit.* ref. 25, **6**, 149 (1961).
- <sup>100</sup> B. Hoffmann, *Phys. Rev.* **121**, 337 (1961).
- <sup>101</sup> Goldenberg, Kleppner, and Ramsay, *Phys. Rev. Lett.* **5**, 361 (15.X.1960).
- <sup>102</sup> N. F. Ramsay, *Rev. Sci. Instr.* **28**, 58 (1956).
- <sup>103</sup> N. F. Ramsay, *Electronics* **33**, 136 (1960).
- <sup>104</sup> Gordy, Tramborulo, and Smith, *Microwave Spectroscopy*, 1953.
- <sup>105</sup> C. Townes and A. Schawlow, *Microwave Spectroscopy*, McGraw-Hill, N.Y., 1955.



<sup>106</sup> Bonanomi, de Prins, and Kartashoff, *Ann. Franc. de chronom.*, 1960, p. 137.

<sup>107</sup> J. R. Wittke, *Pros. IRE* **45**, 291 (1957).

<sup>108</sup> G. V. Skrotskii and T. G. Izyumova, *Usp. Fiz. Nauk* **73**, 423 (1961), *Soviet Phys. Uspekhi* **4**, 177 (1961).

<sup>109</sup> G. Goudet, *L'onde électrique* **38**, 671 (1958).

<sup>110</sup> *Missiles and Rockets*, No. 1, 1961, p. 34.

<sup>111</sup> N. G. Basov and A. P. Petrov, *op. cit.* ref. 25, **3**, 298 (1958).

<sup>112</sup> N. G. Basov and A. M. Prokhorov, *Vestnik (Herald)*, Academy of Sciences U.S.S.R. No. 4, 110 (1960).

<sup>113</sup> Basov, Nikitin, and Osipov, Report, *Phys. Inst. Acad. Sci.*, 1959.

Translated by J. G. Adashko